ELSEVIER

Contents lists available at ScienceDirect

Estuarine, Coastal and Shelf Science

journal homepage: www.elsevier.com/locate/ecss



The influences of phenology, spatial distribution, and nitrogen form on Long Island Sound phytoplankton biomass and taxonomic composition

Zabdiel Roldan Ayala^{a,b}, Stephen A. Arnott^c, Mariapaola Ambrosone^b, Jessica I. Espinosa^{b,d}, Georgie E. Humphries^{a,b}, Maria Tzortziou^e, Joaquim I. Goes^f, Dianne I. Greenfield^{b,a,*}

- ^a School of Earth and Environmental Sciences, Queens College, 65-30 Kissena Blvd, Queens, NY, 11367, USA
- ^b Advanced Science Research Center at the Graduate Center, 85 St Nicholas Terrace, New York, NY, 10031, USA
- ^c Department of Biology, Queens College, 65-30 Kissena Blvd, Queens, NY, 11367, USA
- d Department of Ecology and Evolutionary Biology, University of Connecticut, Storrs, CT, 06269, USA
- e Earth and Atmospheric Science, Center for Discovery and Innovation, The City College of New York, 85 St Nicholas Terrace, New York, NY, 10031, USA
- f Columbia Climate School, Lamont-Doherty Earth Observatory, Columbia University, 630 W. 168th St., New York, NY, 10032, USA

ARTICLE INFO

Keywords: Nitrogen Long Island Sound Phytoplankton Marine ecology Water quality Urbanization

ABSTRACT

Long Island Sound (LIS), USA, is an urban estuary that receives excessive nitrogen (N) inputs resulting in ecosystem impairments, such as hypoxia and algal blooms. Despite established linkages between N concentrations and algal blooms worldwide, connections between N forms and phytoplankton assemblages within LIS remain less characterized, representing a critical information gap for water quality management. This study assessed the spatio-temporal distributions of phytoplankton biomass and abundances, N, and other key water quality parameters Mar-2020 to Oct-2021 in Western (WLIS), Central (CLIS), and Eastern LIS (ELIS). During both study years, mean dissolved inorganic N (DIN) concentrations were significantly higher during fall than other seasons (ANOVA: p < 0.004), coincident with diatom blooms. Diatoms were abundant throughout the study, though WLIS flagellate numbers rose during Jul and Aug both years. Smaller (<5 µm diameter) cells generally contributed most to overall chlorophyll a (Chl a) and with significantly higher summer biomass in WLIS and CLIS than other seasons (ANOVA; WLIS: p < 0.004; CLIS: p < 0.006). Across LIS, there was a clear west to east decline in levels of Chl a, DIN, and the proportional contribution of picoplankton to overall phytoplankton biomass; however, seasonal mean concentrations of Chl a, nutrients, and other water quality parameters did not significantly differ between sampling (0.5 and 2 m) depths except for ELIS summer temperature and Chl a (T-test; both p = 0.002). Given climate change challenges, such as warmer temperatures enhancing blooms particularly in systems enriched with anthropogenic N, findings indicate that N-management strategies should re-evaluate targets spanning LIS. Study results are likely applicable to other eutrophic urban estuaries worldwide.

1. Introduction

Long Island Sound (LIS), the third-largest estuary in the United States (US) in terms of water volume, is bordered by extensive land development that is home to > 11 million people, making it one of the most urbanized estuaries worldwide (Gay et al., 2004; Latimer et al., 2014; US Census Bureau, 2020; Zajac et al., 2020). The estuary is bordered by Connecticut (CT) on the north, New York City (NYC) on the west, and Long Island, NY, to the south. It spans 177×34 km (length x width), has a mean depth of 20 m (Wolfe et al., 1991; Gay et al., 2004), and receives freshwater from 18 rivers, with the Connecticut River contributing 70%

of this riverine input (Vlahos et al., 2020); the eastern end connects to and mixes water with the Atlantic Ocean (Wolfe et al., 1991; Vlahos et al., 2020). LIS supports numerous ecosystem services such as fisheries, recreational, and commercial shipping activities (Krauter et al., 2009; Latimer et al., 2014).

LIS is enriched with nitrogen (N), with primary sources including combined sewage overflows (CSOs), rivers, atmospheric deposition, groundwater, and remineralization (Latimer et al., 2014; Tamborski et al., 2017; Vlahos et al., 2020). Total N (TN) loadings are particularly elevated in Western LIS (WLIS) relative to Central or Eastern LIS (CLIS, ELIS, respectively) by surface runoff and point source CSO inputs from

^{*} Corresponding author. Advanced Science Research Center at the Graduate Center: 85 St Nicholas Terrace, New York, NY, 10031, USA. *E-mail address:* dgreenfield@gc.cuny.edu (D.I. Greenfield).

NYC (Vaudrey, 2017; Vlahos et al., 2020), leading to seasonal (summer) hypoxia (Anderson and Taylor, 2001; Swanson et al., 2016; Vaudrey, 2017; CTDEEP, 2021; Humphries et al., 2023). Much of the CSO-sourced TN enters LIS from the East River, which contributes a mean (standard error) of 3.2 (2.2) $\times\,10^6$ kg y^{-1} towards WLIS's TN (Vlahos et al., 2020). Further east, the combined freshwater discharge of the Connecticut, Housatonic, Thames and Quinnipiac rivers varies seasonally, with springs characterized by higher discharge rates $(2.4 \times 10^8 \text{ m}^3 \text{ d}^{-1})$ than summers $(2.0 \times 10^7 \text{ m}^3 \text{ d}^{-1})$ (Gobler et al., 2006). N discharge from surrounding rivers to LIS varies spatially where 2.6 (0.8) \times 10⁶ kg y⁻¹ enters WLIS, 4.7 (1.3) \times 10⁶ kg y⁻¹ enters CLIS, and 14.2 (2.7) \times 10⁶ kg y⁻¹ enters ELIS with 10.8 (8.9) \times 10⁶ kg y⁻¹ exported to the Atlantic Ocean (Vlahos et al., 2020). Hypoxia was initially observed in LIS during 1974 (Parker and O'Reilly, 1991; Lee and Lwiza, 2008) and has recurred annually since 1987, when monitoring efforts began (Parker and O'Reilly, 1991; Vaudrey, 2017). Upgrades to wastewater treatment facilities over the past decade to meet total maximum daily load (TMDL) targets have lowered point-source TN inputs (NYSDEC and CTDEEP. 2000; Whitney and Vlahos, 2021), thereby reducing hypoxia duration, intensity (Bennett et al., 2000; Lee and Lwiza, 2008; Latimer et al., 2014), and coverage (63% area reduction from 2006 to 2016; Whitney and Vlahos, 2021).

Both the concentrations (0.6 mg L^{-1} of yearly mean TN at WLIS on 2017; Vlahos et al., 2020) and chemical form(s) of dissolved N, as well as phosphorus (P), influence LIS phytoplankton assemblage structure (Anderson and Taylor, 2001; Suter et al., 2014). Diatom blooms are generally enhanced by dissolved inorganic N (DIN), especially nitrate (NO_3^-) , due to their rapid uptake rates of oxidized N (Bronk et al., 2007; Heil et al., 2007). Similarly, in LIS NO₃ has been experimentally shown to increase diatom abundances (Gobler et al., 2006; Brown and Greenfield, 2022) and fuel winter-spring diatom blooms in the field (George et al., 2014). Reduced N forms, such as ammonium (NH₄), enhance cell growth rates of other phytoplankton taxa, such as harmful algal bloom (HAB) forming dinoflagellates (e.g., Alexandrium catenella, Dinophysis spp.) and euglenoids (Hattenrath-Lehmann et al., 2010, 2015; Tossavainen et al., 2019). By comparison, other regional HAB species (e.g., Prorocentrum minimum, Margalefidinium polykrikoides, Aureococcus anophagefferens) and cyanobacteria take up dissolved organic nitrogen (DON) faster than DIN, offering them an advantage when DIN becomes limited (Lomas et al., 2004; Nuzzi and Waters, 2004; Heisler et al., 2008; Gobler et al., 2012; Griffith et al., 2019a). Since smaller-celled phytoplankton species can outcompete larger-celled species for DIN due to their relatively greater nutrient uptake efficiency (Suter et al., 2014), environments with lower DIN levels could provide scenarios where prior TN reductions to achieve N management targets shift phytoplankton community composition toward smaller cells. These assemblage shifts may influence estuarine food webs. For example, grazing of LIS phytoplankton by zooplankton (copepods, ciliates, other heterotrophic microplankton) can affect seasonal phytoplankton community structure (Mariani et al., 2013; George et al., 2014); this may be more pronounced in the eastern LIS regions because zooplankton play a lesser role in controlling phytoplankton biomass within the Lower Hudson River (near WLIS) than CLIS (Lonsdale et al., 1996; George et al., 2014). Given the broad impacts of TN loadings on LIS water quality, it is critical to identify how individual N-forms influence phytoplankton assemblages, laying a foundation for additional research exploring broader trophic dynamics.

In addition to the chemical form of N, phytoplankton assemblages often vary with depth within a water body. In LIS, seasonal stratification is driven by thermocline development, typically $\sim \! 10$ m, that is enhanced by greater salinity with depth, though ELIS stations close to the Atlantic Ocean often exhibit weak summer thermoclines, reducing stratification in this basin (Latimer et al., 2014; CTDEP, 2021). Stratification across LIS is minimal Oct-Jan, starts to develop near the end of Feb, then accelerates in Apr until reaching its maximum Jul–Aug (Latmier et al., 2014) with interannual variability of temperature and

salinity within the water column associated with water property fluctuations by the shelf slope (Lee and Lwiza, 2005). This relates to phytoplankton assemblages because globally, phytoplankton biomass is often concentrated at the sub-chlorophyll maximum (SCM) (Cullen, 2015) as certain taxa, such as diatoms, tend to occupy deeper depths whereas cyanobacteria, dinoflagellates, and other flagellates typically reside above the SCM due to adaptations that maximize utilization of physical features in surface waters (temperature, light) for photosynthesis and growth while minimizing loss (Figueiras and Pazos, 1991; Latasa et al. 2016a, 2016b). Less is known about the current spatial patterns (vertical and horizontal) of LIS phytoplankton assemblages. Elucidating differences in water quality (N form, temperature, light, etc.) among depths will help identify the primary drivers of LIS phytoplankton biomass, species composition, and spatio-temporal distributions. This information can inform ecological and biogeochemical models, bloom forecasting, as well as other in situ and remotely sensed surface water-quality measurements to improve N-management decisions.

Over a typical year, phytoplankton population dynamics in LIS and adjacent embayments mirror patterns characteristic of temperate estuaries with diatoms, particularly Skeletonema, Thlassiosira, Dactyliosolen, Asterionellopsis, and Leptocylindrus (Greenfield et al., 2005; George et al., 2014; Latimer et al., 2014), abundant year-round. Commonly-observed dinoflagellates in LIS, such as Gonyaulax spp., Dinophysis acuminata, Prorocentrum spp., and Alexandrium spp., become relatively more numerous during summers (Conover et al., 1954; Wikfors, 2005; Liu and Lin, 2008; Latimer et al., 2014). The most abundant cyanobacterial genus in LIS is Synechococcus, with other phytoplankton taxa (e.g., raphidophytes, cryptophytes, chlorophytes, euglenophytes, silicoflagellates, and chrysophytes) typically co-occurring at lower levels (Latimer et al., 2014). Understanding how N form influences LIS phytoplankton phenology will shed important insight to the biogeochemical processes that regulate seasonal blooms and exacerbate HABs. The goal of this project was to evaluate the inter-annual vertical and horizontal (within depth) distributions of phytoplankton assemblages and biomass across LIS as they relate to key physical and biogeochemical metrics. Two hypotheses were tested: Hypothesis 1) In the most urbanized (WLIS) region, seasons with elevated NO_3^- + nitrite (NO_2^-) levels will coincide with higher diatom cell concentrations compared to CLIS and ELIS while seasons with high NH₄⁺ levels will be associated with more frequent and cell dense dinoflagellate blooms. Hypothesis 2) Phytoplankton biomass (mostly >20 µm cell diameter) and dinoflagellate abundances will be higher in sub-surface (0.5 m) than surface (2 m) depths during summers, coincident with well-lit, warmer subsurface waters. These hypotheses were tested by evaluating phytoplankton species composition, abundances, and biomass of three different cell size fractions as well as relevant physical (salinity, light, temperature and DO) and nutrient (primarily N) parameters across LIS over a two-year period.

2. Methods

2.1. Sample collection

The Connecticut Department of Energy and Environmental Protection (CTDEEP) conducts biweekly (May–Sept) and monthly (Apr–Oct) LIS water quality and hypoxia monitoring surveys from sub-surface (~0.5 m), surface (~2 m), and bottom (–5 m from the benthos) depths. This project leveraged CTDEEP long-term survey efforts (9-Mar-20 to 5-Oct-21) (Fig. 1), emphasizing WLIS due to the region's higher N inputs and susceptibility to eutrophic and hypoxic conditions relative to CLIS and ELIS (Anderson and Taylor, 2001; Vlahos et al., 2020). Due to social distancing and related restrictions from the COVID-19 pandemic, 2020 sample collection was not possible prior to Jul for WLIS and CLIS or from additional depths. Accordingly, water samples were collected using Niskin bottles (5 L) affixed to a rosette from subsurface (0.5 m) and

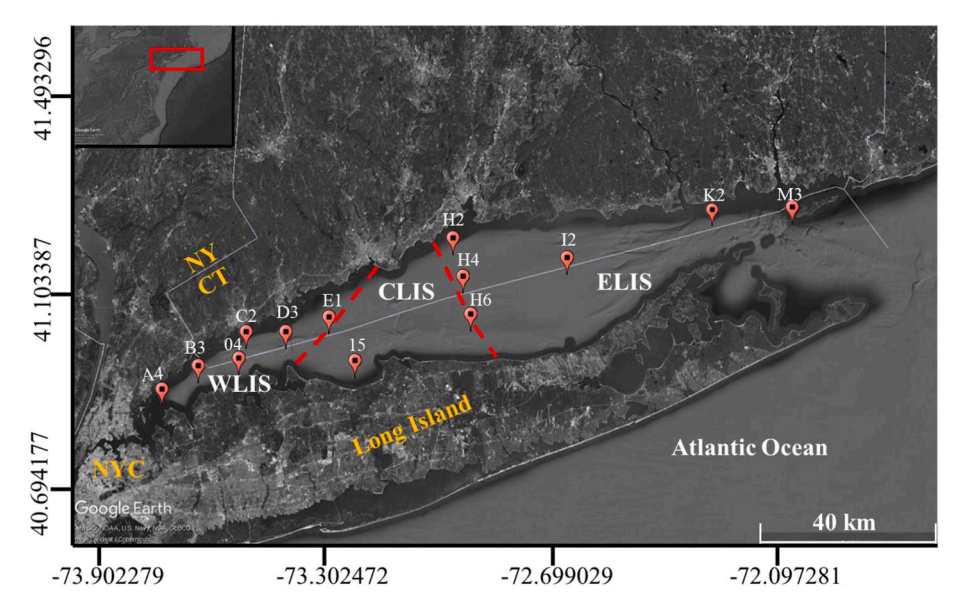


Fig. 1. Map of Long Island Sound (LIS) US showing Connecticut Department of Energy and Environmental Protection (CTDEEP) sampling stations (Mar 2020 to Oct 2021). WLIS = Western Long Island Sound, CLIS = Central Long Island Sound, and ELIS = Eastern Long Island Sound, NY = New York, CT = Connecticut, NYC = New York City. Insert shows northeast coast of the USA.

surface (2 m) depths to target high light-adapted phytoplankton and coincide with long-term data, respectively, and then dispensed in to separate clean 1 L amber NalgeneTM bottles (n=3 per station and depth). Physical water quality data were courtesy of CTDEEP measurements of temperature (°C), dissolved oxygen (DO, mg L⁻¹), salinity, and pH using a YSI EXO2 data sonde in addition to Secchi disk depths (m), which were used to calculate extinction coefficients (k) as k=1.7/(Secchi disk depth). After each survey, samples were transported by vehicle (\sim 2 h) to the laboratory then processed immediately. Data from CLIS stations H4 and H6 were pooled due to their limited samples and close proximity.

2.2. Nutrients

Water samples were gently rotated ~10x to ensure they were wellmixed. To sample for total dissolved nitrogen (TDN) and phosphorus (TDP), ~17–18 mL from each replicate were syringe-filtered through 25 mm, 0.7 µm pore size Whatman® glass fiber filters (GF/Fs) such that filtrate was collected in 20 mL (previously soaked for >24 h with 10% hydrochloric acid (HCl) then rinsed 3x with analytical-grade deionized water) glass scintillation vials. Dissolved inorganic N (DIN) as NO₃ + NO₂, and ammonia-N (NH₄⁺⁺ ammonia (NH₃); henceforth the primary form, NH₄), as well as dissolved inorganic P (DIP) as orthophosphate (PO_4^{3-}) , were similarly filtered then stored $(-20 \, ^{\circ}\text{C})$ until analysis. Dissolved organic N (DON) and P (DOP) were calculated per replicate as TDN-DIN and TDP-DIP, respectively. Silicate (Si) samples were similarly filtered, with filtrate stored in plastic scintillation vials. Concentrations for each nutrient were analyzed using a Lachat QuickChem 8500 following standard methods (Parsons et al., 1984; Grasshoff et al., 1999). If measured concentrations fell below the limits of detection (LOD), those LOD values were substituted as follows: $0.05 \mu M (NH_4^+)$, $0.014 \ \mu M \ (NO_3^- + NO_2^-), \ 0.0646 \ \mu M \ (PO_4^{3-}) \ and \ 0.2 \ \mu M \ (Si) \ (Lachat$ Instruments, 2019).

2.3. Chlorophyll a

Chlorophyll *a* (Chl *a*) concentrations were measured as a proxy of phytoplankton biomass using standard acetone-extraction procedures (Welschmeyer, 1994). To collect Chl *a* samples, 40 mL from each field replicate were passed through GF/F filters by vacuum filtration (5

mmHg). This procedure was performed for three cell size fractions: total (no filtration), $<\!20~\mu m$, and $<\!5~\mu m$ (filtrate passed through 20 μm or both 20 μm and 5 μm Nitex® meshes, respectively) to determine the relative contributions of microplankton ($>\!20~\mu m$), nanoplankton (5–20 μm), and small nanoplankton and picoplankton ($<\!5~\mu m$) to overall Chl a. Each filter was then placed inside a 20 mL plastic scintillation vial and frozen ($-20~^\circ C$) until extraction using 7 mL of high-performance liquid chromatography (HPLC)-grade acetone (90%) dispensed into each vial. Samples were then briefly (1–2 s) vortex mixed and stored ($-20~^\circ C$) for 36–48 h. Afterward, 2–3 mL of acetone-extracted pigments were dispensed into Thermo-Fisher^TM disposable borosilicate glass culture tubes, and Chl a concentrations (μg L $^{-1}$) were measured using a Turner Trilogy fluorometer with Anacystis nidulans as a pigment standard following manufacturer specifications.

2.4. Phytoplankton community composition

Aliquots of water from each replicate were dispensed in to 20 mL amber glass vials, preserved using Lugol's iodine solution to a 15% or 1% volumetric dilution (depending of the strength of Lugol's solution), then stored (4 $^{\circ}$ C) until analysis. To quantify phytoplankton community composition, individual cells from each preserved replicate were identified to the lowest taxonomic level possible using a 1 mL Sedgewick rafter chamber and an Olympus (BX53) compound light microscope (10X objective) or a Nikon Eclipse Ti2 (Nikon) inverted microscope (10X or 20X objective). Species composition was determined by counting a minimum of 300 cells or the whole chamber, whichever occurred first. Cell concentrations were corrected for dilution during preservation (LeGresley and McDermott, 2010).

2.5. Data analyses

Statistical analyses were performed using R 4.2.0 within R Studio 2022.02.3 (R Studio Team, 2022; R Core Team, 2022). Paired T-tests were used to evaluate whether variables differed consistently between 0.5 m and 2 m depth measurements. For each sampling event (i.e., 0.5 m and 2 m measurements collected on any single station/date), the mean 2.0 m value was subtracted from the mean 0.5 m value. These differences were averaged per sampling date, and data from all sampling dates were then tested for deviation from zero (H0: no difference between 0.5

m and 2 m values). Since thirteen variables were tested, a Bonferroni-adjusted significant level of $\alpha=0.004$ was used (i.e., 0.05/13).

To test whether 0.5 m measurements varied with season (defined as solar seasons bounded by solstice and equinoxes), Analysis of Variance (ANOVA) mixed models were implemented with season as a fixed factor

and sampling date as a random factor (lme4 package; Bates et al., 2015). The 0.5 m depth was selected for this analysis because prior tests indicated that the two studied depths often had similar water quality and phytoplankton biomass. Response variables (WLIS and CLIS: Chl a, NH $_{+}^{+}$, NO $_{2}^{-}$ + NO $_{3}^{-}$, PO $_{4}^{-}$, Si, temperature, salinity, pH and DO; WLIS: DOP, DON) were initially Box-Cox transformed to meet normality criteria

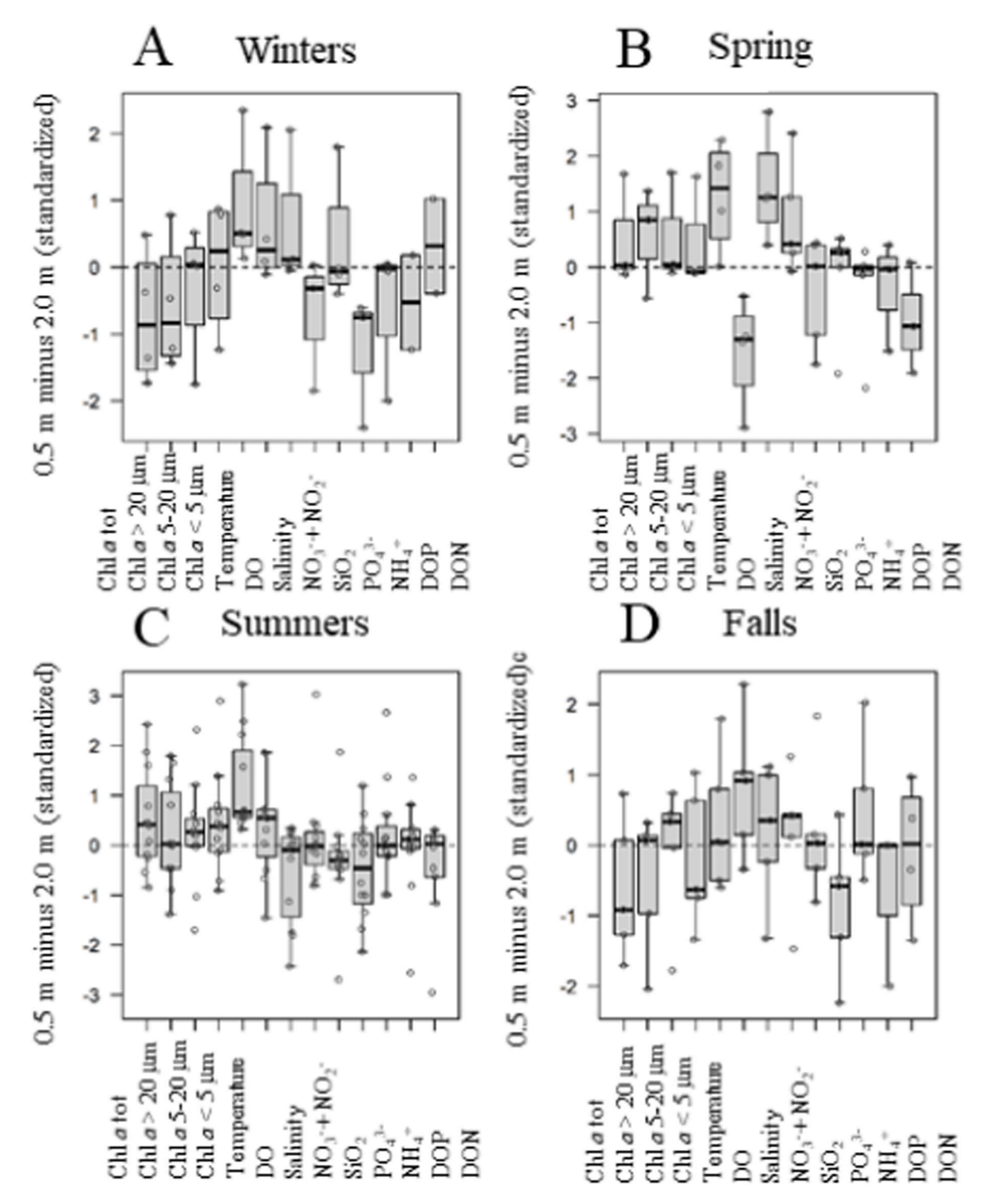


Fig. 2. Box plots showing differences between the median, 25th and 75th percentiles (with inter-quartile range) between 0.5 m and 2 m depths for key water quality parameters across Long Island Sound: Chlorophyll a (Chl a) (total (tot), >20 μ m, 5–20 μ m, and <5 μ m cell size fractions), temperature, dissolved oxygen (DO), salinity, nitrate + nitrite (NO $_3^-$ + NO $_2^-$), silicate (SiO $_2$), phosphate (PO $_3^+$), ammonium (NH $_4^+$), dissolved organic phosphorus (DOP) and nitrogen (DON) across seasons (determined by solstice and equinoxes): winters (A), summers (B), spring (C) and falls (D). Note: Plots have different (compared to text) nomenclature for inorganic nutrients due to limitations with subscripts and size in R.

(MASS package; Venables and Ripley, 2002). Seasonal differences were tested in WLIS and CLIS, but not ELIS because that region was sampled too infrequently. Since multiple variables were analyzed per region, the significance level was adjusted to $\alpha=0.004$ for WLIS (0.05/13 tests), and 0.006 for CLIS (0.05/8 tests). If a significant seasonal effect was detected, pairwise comparisons between seasons were performed using the emmeans function with a Bonferroni correction factor (emmeans package; Lenth, 2022).

A principal component analysis (PCA) was used for exploring relationships between 0.5 m measurements of Chl a (all size fractions), nutrients, and water quality in WLIS, where the most samples and thus corresponding data were available from. The PCA was implemented on scaled Box-Cox transformed data using the prcomp function of the R stats package, and a biplot of PC1 and PC2 was generated using the ggbiplot function of the ggbiplot package.

3. Results

3.1. Physical water quality

Across WLIS and CLIS, temperature and dissolved oxygen (DO) levels were inversely related (Tables 1, S1), with higher DO concentrations associated with cooler months and vice versa, consistent with greater oxygen solubility at colder temperatures. Mean temperature and DO (0.5 m) levels in WLIS and CLIS were significantly different among seasons (ANOVA, WLIS temperature: F=16.18, p<0.004 and DO: F=9.33, p=0.02; CLIS temperature: F=254.57, p<0.006 and DO: F=31.98, p=0.006), with mean WLIS summer temperature significantly higher than other seasons (pairwise comparisons, Summer, 2020-Fall, 2020: p=0.002, Winter, 2021- Summer, 2021: p=0.001). Neither salinity nor pH differed significantly among seasons (ANOVA, WLIS; salinity: F=3.17, p=0.08, pH: F=1.27, p=0.34. CLIS; salinity: F=0.46, p=0.71, pH: F=0.48, p=0.67). No distinct seasonal trends were observed for light extinction coefficients within any LIS region (Table S1).

Across regions and within season, some physical parameters were comparable, such as temperature, surface DO and pH (Table S1). By comparison, salinity increased west to east with greater oceanic exchange, such that values closer to 26 were more common in WLIS while

salinities closer to 30 were more typical of ELIS (Tables 1, S1) except for station D3 on 22-Oct-20, when a salinity of 30–31 was recorded at both depths. The light extinction coefficient generally decreased (greater water clarity) west to east.

Mean physical water quality parameters were not significantly different between depths throughout the study except for temperature during both summers (Figs. 2 and 3; Tables 1, S1), when 0.5 m was significantly warmer than 2 m (T-test, p=0.002). This was largely attributed to a prominent thermocline that developed within WLIS, as mean summer temperatures were $\geq 0.2~^{\circ}\text{C}$ warmer at 0.5 m than 2 m both years for any given station/date (Table 1). In both CLIS and ELIS, temperature was comparable between sampling depths (Figs. 2 and 3; Table S1). No significant differences between depths were found for mean pH, DO, or salinity throughout the study period (T-test, p>0.004 for all parameters).

3.2. Nutrients

3.2.1. DIN

Levels of $NO_3^- + NO_2^-$ remained low (<2.0 μ M) from spring through mid-summers across LIS (Fig. 4, S1-3). However, during 2020 mean $NO_3^- + NO_2^-$ concentrations at A4 and B3 rose from <1.1 μ M during late summer (1-Sep) to fall (12-Oct to 6-Nov), reaching mean (standard error) concentrations between 3.7 (0.5) μ M and 10.0 (0.3) μ M (Fig. 4, S1). Similarly, in WLIS mean $NO_3^- + NO_2^-$ concentrations (0.5 m) differed across seasons (ANOVA, F=11.57, p<0.004), with fall 2021 concentrations significantly higher (pairwise comparison, p=0.002) than summer 2021, coincident with elevated fall diatom abundances. In both ELIS and CLIS, $NO_3^- + NO_2^-$ concentrations remained <3.2 (1.2) μ M throughout the sampling period with no significant differences between seasons in CLIS (Figs. S2 and S3) (ANOVA, F=0.28, p=0.83). Regional mean $NO_3^- + NO_2^-$ concentrations were similar between depths throughout the study (Figs. 2 and 3) (T-test, WLIS: p=0.56; CLIS: p=0.94, ELIS: p=0.44).

During both study years, concentrations of NH $_{+}^{+}$ increased from summer to fall in WLIS in contrast to CLIS and ELIS (Fig. 4, S1-3). For example, during 2020 in WLIS mean NH $_{+}^{+}$ concentrations at A4 (0.5 m depth) on 1-Sep were 0.8 (0.5) μ M then rose to 11.0 (0.7) μ M by 6-Nov with pooled fall 2020 NH $_{+}^{+}$ concentration means significantly higher

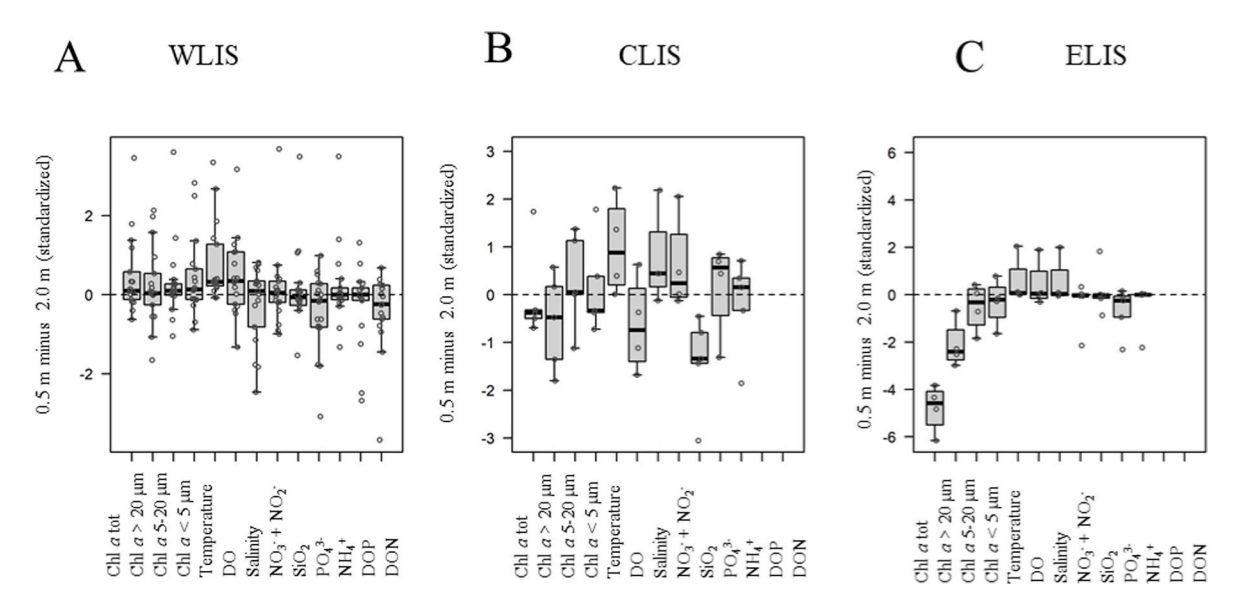


Fig. 3. Box plots showing differences between the median, 25th and 75th percentiles (with inter-quartile range) between 0.5 m and 2 m depths for key water quality parameters in Long Island Sound: Chlorophyll a (Chl a) (total (tot), >20 μ m, 5–20 μ m, and <5 μ m cell size fractions), temperature, dissolved oxygen (DO), salinity, nitrate + nitrite (NO $_3^-$ + NO $_2^-$), silicate (SiO $_2$), phosphate (PO $_3^+$), ammonium (NH $_4^+$), dissolved organic phosphorus (DOP) and nitrogen (DON) across region: Western Long Island Sound = WLIS (A), Central Long Island Sound = CLIS (B) and Eastern Long Island Sound = ELIS (C). Note: Plots have different (compared to text) nomenclature for inorganic nutrients due to limitations with subscripts and size in R.

Table 1 Sampling dates (season-year) and site with their respective means (of n measurements) and ranges for physical water quality parameters in Western Long Island Sound: Temp (°C) = Temperature, Sal = Salinity, DO (mg L⁻¹) = Dissolved Oxygen obtained from ship surveys. Separate n values are provided for k (m⁻¹) = Extinction Coefficient because Secchi depths were not always measured. Values correspond to 0.5 m (bold) and 2 m (unbold) depths. Seasons are abbreviated as Summer = Sum, Fall = Fal, Winter = Win and Spring = Spr. Dashed line (–) indicates that data and/or ranges were unavailable for that station/date.

Water Quality												
Season		Тетр		Sal		DO		pH		<u>k</u>		
	Site(n)	Mean	Range	Mean	Range	Mean	Range	Mean	Range	Mean	n	Range
Sum 2020	C2 (4)	23.25	22.02-24.36	26.72	25.65-27.58	7.76	6.98-9.62	8.09	7.99-8.17	0.91	3	1.00-0.85
	*C2 (4)	23.22	22.11-24.29	26.77	25.99-27.60	7.61	6.45-9.10	8.05	7.96-8.18	1.00	3	1.06-0.89
	B3 (5)	24.17	21.79-25.35	27.02	26.53-28.27	8.42	7.24-9.79	8.16	7.82-8.27	1.08	4	1.13-0.89
	B3 (4)	23.77	24.04-24.94	26.68	26.51-27.12	9.10	6.29-9.79	8.20	7.84-8.28	1.08	4	1.13-0.89
	A4 (4)	23.25	21.37-24.96	26.58	26.37-26.69	7.45	6.71-7.79	8.11	7.88-8.31	1.09	3	1.13-1.06
	*A4 (3)	22.95	21.26-26.45	26.47	26.23-27.12	7.29	6.29-8.27	7.92	7.67-8.13	1.09	3	1.13-1.06
	04 (4)	24.31	21.49-26.45	26.95	26.71-26.96	7.93	7.67-9.79	8.18	8.03-8.40	0.98	3	1.30-0.94
	*04 (3)	23.71	21.02-25.03	26.72	26.57-27.07	8.69	8.03-9.79	8.15	8.00-8.35	0.98	3	1.30-0.94
	D3 (4)	23.89	19.42-26.41	27.28	26.97-28.98	7.40	7.09-7.73	8.11	7.84-8.22	1.08	4	1.13-1.06
	D3 (4)	22.95	19.13-24.82	27.35	27.15-27.64	6.98	6.68-8.55	7.83	7.83-8.20	1.08	4	1.13-1.06
Fal 2020	C2 (1)	18.60	_	28.43	_	7.84	-	7.94	-	0.89	1	-
	*C2 (1)	18.61	_	28.50	_	7.29	-	7.86	_	0.89	1	-
	B3 (2)	15.78	13.48-18.08	27.62	27.26-27.97	8.20	8.05-8.35	8.20	7.94-8.35	0.91	2	1.31-0.91
	*B3 (2)	15.73	13.35-18.10	27.59	27.18-28.00	8.10	7.57-8.62	8.17	7.87-8.47	0.91	2	1.31-0.91
	A4 (2)	15.79	13.67-17.91	26.97	26.63-27.30	8.60	7.76-9.43	8.32	7.83-8.80	0.71	2	0.89-0.71
	A4 (2)	15.77	13.62-17.92	26.90	26.52-27.27	7.84	7.48-8.20	8.28	7.79–8.77	0.71	2	0.89 - 0.71
	D3 (3)	17.04	14.42-18.83	29.36	28.27-30.92	9.14	7.73-10.84	8.01	7.82-8.29	0.64	2	0.71-0.57
	D3 (3)	16.92	14.45-18.63	29.26	28.29-31.02	7.85	7.52-8.46	7.88	7.81-7.92	0.64	2	0.71 - 0.57
Win 2021	C2 (1)	2.61	-	27.53	_	12.32	-	8.02	-	0.34	1	-
	*C2 (1)	2.54	-	27.47	_	10.56	-	8.12	_	0.34	1	-
	B3 (1)	3.05	_	26.91	_	12.99	-	8.16	_	0.56	1	-
	B3 (1)	2.98	-	26.79	_	12.67	-	8.22	_	0.56	1	-
	A4 (1)	3.27	_	26.59	_	13.15	_	8.11	_	0.68	1	_
	A4 (1)	3.04	_	26.60	_	12.84	_	8.24	_	0.68	1	_
	D3 (1)	3.09	_	27.47	_	11.83	_	8.18	_	0.37	1	_
	*D3 (1)	3.02	_	27.47	_	11.87	_	8.15	_	0.37	1	_
Spr 2021	C2 (2)	12.27	6.45-18.08	27.01	26.47-27.54	9.18	8.77-9.59	_	_	0.53	2	0.65-0.40
	*C2 (3)	11.23	6.11-17.29	26.90	26.42-27.20	9.97	9.61-10.54	_	_	0.53	2	0.65-0.40
	B3 (2)	14.40	10.41-18.38	26.13	26.01-26.25	10.40	8.94-11.86	_	_	0.85	1	_
	B3 (3)	11.90	7.77-17.62	26.35	25.95-26.86	10.84	9.44-12.84	_	_	0.85	1	_
	A4 (2)	12.93	8.23-17.62	26.09	26.04-26.13	10.33	9.34-11.32	_	_	0.84	1	_
	A4 (3)	11.55	8.02-15.75	26.16	25.86-26.44	9.71	7.57-12.45	_	_	0.84	1	_
	D3 (2)	14.08	8.52-19.64	27.02	26.97-27.06	10.07	8.99-10.65	-	_	0.74	1	_
	*D3 (3)	11.77	7.42-17.69	26.92	26.58-27.15	10.09	9.59-10.67	_	_	0.74	1	_
Sum2021	C2 (5)	23.02	21.63-24.27	26.62	25.94-26.83	8.06	7.42-9.01	7.88	7.80-7.93	1.05	5	1.31-0.77
	C2 (5)	22.83	21.24-23.86	26.62	25.86-26.81	7.48	7.29-7.82	7.90	7.83-7.96	1.05	5	1.31-0.77
	B3 (5)	23.66	22.56-25.28	26.11	25.34-26.49	8.37	7.66-9.12	7.98	7.89-8.03	1.14	5	1.42-0.85
	*B3 (5)	23.36	22.40-24.33	26.10	25.32-26.57	8.46	7.87-9.43	7.95	7.87-8.04	1.14	5	1.42-0.85
	A4 (5)	23.26	22.07-24.50	25.69	25.07-26.31	7.94	6.66-9.25	7.81	7.55-8.01	1.18	5	1.42-1.06
	*A4 (5)	23.05	21.76-23.98	25.71	25.11-26.21	7.04	4.61-9.35	7.77	7.45-8.02	1.18	5	1.42-1.06
	D3 (5)	23.58	22.18-24.81	26.33	25.57-26.99	8.41	7.55-9.49	7.97	7.90-8.04	1.00	5	1.06-0.85
	D3 (5)	23.19	22.11-24.64	26.55	25.94-26.94	8.19	7.70-8.97	7.96	7.93-7.98	1.00	5	1.06-0.85
	04 (4)	23.86	22.09-25.32	25.94	25.37-26.49	8.52	7.70-9.80	7.97	7.88-8.01	0.99	5	1.13-0.85
	*04 (5)	23.78	22.03-24.88	26.22	25.56-26.63	8.15	7.58-9.61	7.94	7.87-8.00	0.99	5	1.13-0.85
Fal 2021	C2 (1)	21.31	-	26.77	-	7.46	-	7.85		0.70	1	-
	*C2 (1)	21.40	-	26.87	_	6.57	-	7.84		0.70	1	_
	B3 (1)	21.17	-	26.43	_	8.68	-	7.86		0.85	1	_
	B3 (1)	21.18	-	26.45	_	6.54	-	7.84		0.85	1	_
	A4 (1)	20.85	-	25.73	_	7.64	-	7.91		0.68	1	_
	*A4 (1)	20.92	-	25.75	_	6.89	-	7.87		0.68	1	_
	D3 (1)	21.29	_	26.41	_	7.36	-	7.95		0.85	1	_
	D3 (1)	21.22	_	26.72	_	7.32	_	7.94		0.85	1	_

than winter 2021 (ANOVA, F=11.05, p<0.004). However, concentrations of NH $_4^+$ were higher than NO $_3^-+$ NO $_2^-$ on 7-Jul at A4 (Fig. 4), coincident with a euglenoid bloom. In CLIS, NH $_4^+$ concentrations were lower (<2.0 μ M) throughout the year with no significant differences among seasons (ANOVA, F=2.64, p=0.29) (Fig. S2). ELIS NH $_4^+$ concentrations were very low (<0.5 μ M) throughout the study with the exception of 4-Jun-20 (Fig. S3). Significant differences between depths were not detected for either NO $_3^-+$ NO $_2^-$ (T-test, WLIS: p=0.56; CLIS: p=0.94, ELIS: p=0.44) or NH $_4$ (T-test, WLIS: p=0.43, CLIS: p=0.68, ELIS: p=0.38).

3.2.2. DIF

Throughout the study, concentrations of PO_4^{3-} were <6 μ M across LIS, comparable between WLIS and CLIS (Fig. 4, S1, S2), and exhibited no significant seasonal differences in either WLIS (ANOVA, F=3.16, p=0.04) or CLIS (ANOVA, F=0.24, p=0.85). ELIS waters were characterized by the lowest PO_4^{3-} levels with the highest mean concentrations at H2 (0.5 m), reaching 0.9 (0.3) μ M on 8-Mar-21 (Fig. S3). Concentrations of PO_4^{3-} were not significantly different between study depths (T-test, WLIS: p=0.08, CLIS: p=0.75, WLIS: p=0.20).

3.2.3. DON and DOP

DON contributed the most to the overall dissolved N-pool with WLIS

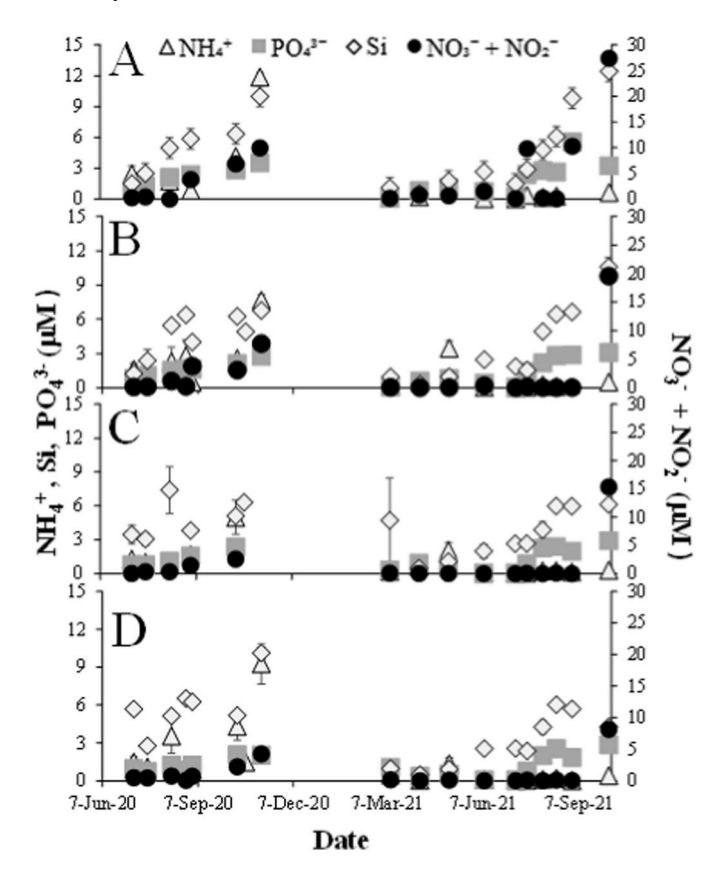


Fig. 4. Mean (n=3) (SE) concentrations (μ M) of dissolved inorganic nutrients: ammonium, nitrate + nitrite, orthophosphate, and silicate (NH₄⁺, NO₃⁻ + NO₂⁻, PO₃⁴, Si, respectively) at 0.5 m depth in Western Long Island Sound (7-Jul-20 to 5-Oct-21) at stations A4 (A), B3 (B), C2 (C), and D3 (D). Secondary axis is for NO₃⁻ + NO₂.

values $> 5.0~\mu M$ (Fig. 5, S4). In WLIS, no significant differences were detected among seasons for either DON or DOP (ANOVA, DON: F=2.44, p=0.10, DOP: F=1.26, p=0.33), though DON concentrations exceeded 150.0 μM on 7-Jul-20 at all stations (Fig. 5). In 2021, peak DON levels (0.5 m) varied across WLIS stations such that highest concentrations occurred at C2 and D3 on 31-Aug and at A4 and B3 on 5-Oct (Fig. 5). DOP values remained low (\leq 2.5 μM) throughout the study period. Neither DON nor DOP concentrations were significantly different between depths (T-test, DON: p=0.10; DOP: p=0.30).

3.2.4. Si

Si concentrations remained <6 μ M throughout LIS during winter through early summer, but increased late summer and fall both years, reaching 6–12 μ M (Fig. 4, S1-S3). In WLIS, lowest Si concentrations (<3 μ M) were observed across all stations and depths from spring to midsummer (Jul) of 2021 before increasing. For example, mean concentrations at A4 (0.5 m) were 4.7 μ M (0.4) on 3-Aug-21 then rose to 12.4 μ M (1.0) by 5-Oct-21. No marked gradients in Si concentrations were observed from WLIS to CLIS/ELIS (Fig. 4, S1-3). Concentrations of Si were not significantly different across seasons in WLIS (ANOVA, F=5.43, P=0.006) or CLIS (ANOVA, F=17.66, P=0.05). Mean concentrations of Si were not significant between depths (T-test, WLIS: P=0.45; CLIS: P=0.03).

3.3. Chlorophyll a

During both study years, seasonal mean total Chl a concentrations in WLIS and CLIS were highest during summers for any given station and depth, reaching 20–30 μ g L $^{-1}$ in WLIS (Fig. 6, S5, S6). Within WLIS, the season with the second highest Chl a concentrations shifted from spring

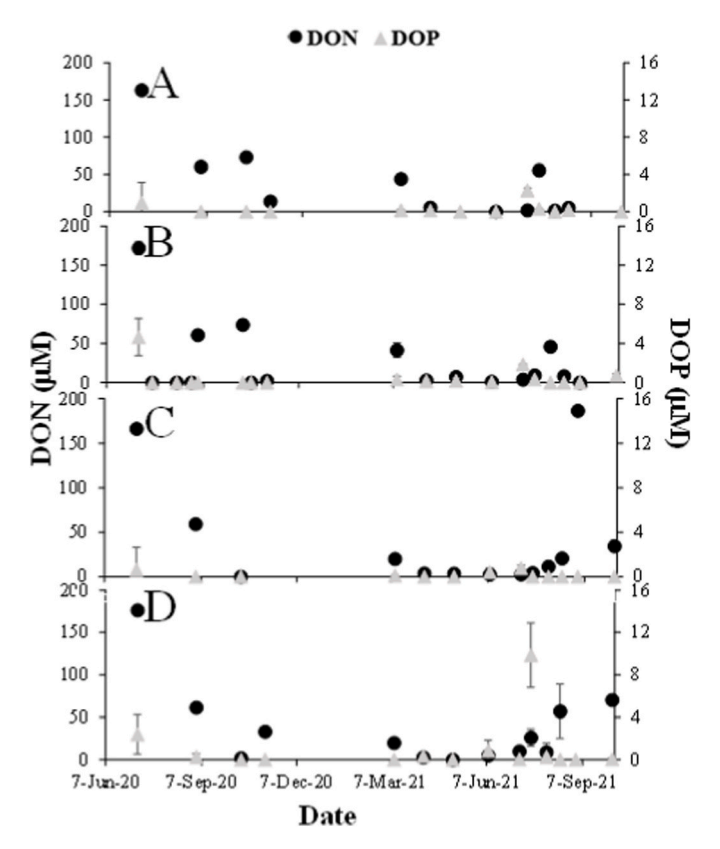


Fig. 5. Mean (n=3) (SE) concentrations (μ M) of dissolved organic nutrients: dissolved organic nitrogen and phosphorus (DON and DOP, respectively) at 0.5 m depth in Western Long Island Sound (7-Jul-20 to 5-Oct-21) at stations A4 (A), B3 (B), C2 (C), and D3 (D). Secondary axis is for DOP.

(A4 and B3) to fall (D3) across a west to east transition. At C2, spring and fall peaks were comparable, coincident with elevated numbers of the chain-forming diatoms *Thalassiosira* and *Leptocylindrus* (Figs. 6C and 7C). A drop in WLIS mean total Chl *a* was observed on 10-May-21, when Chl *a* values were <2.30 μ g L⁻¹ (Fig. 6, S5).

Mean total Chl a concentrations decreased west to east for both sampling depths, along with a diminishing contribution of <5 µm sized cells to total Chl a and an increasing contribution from >20 µm sized cells (Fig. 6, S5, S6). For example, on 16-Aug-21 mean total Chl a concentrations at WLIS station A4 (2 m depth) were 15.91 (0.13) $\mu g L^{-1}$ compared to 7.28 (0.09) $\mu g L^{-1}$ at station D3. This west to east decline became more prominent in CLIS and ELIS where mean Chl a concentrations were $<5 \mu g L^{-1}$ throughout the study (Figs. S5 and S6). Furthermore, in WLIS, the <5 μm size fraction contributed the most Chl a to overall biomass compared to other size classes. For example, at station A4 (3-Aug-21, 0.5 m depth), the <5 μm size fraction comprised $25.32\,(1.41)\,\mu g\,L^{-1}$ (75%) of total Chl $\emph{a}.$ Across CLIS and depths, the ${<}5$ μm fraction contributed the most to total Chl a during late spring and summer while microplankton (>20 μm) contributed more during fall and early spring (Fig. S6). Chl a concentrations for the <5 μm size fraction were significantly higher during summer than other seasons in both CLIS and WLIS (ANOVA, WLIS: F = 11.73, p < 0.004; CLIS: F = 11.73137.65, p < 0.006) (pairwise comparison, WLIS; Summer, 2020- Fall, 2020: p = 0.002, Winter, 2021- Summer 202: p = 0.002). Across ELIS, the >20 µm (microplankton) size fraction was the greatest Chl α portion (e.g., 60% at I2, 0.5 m, 9-Mar-20) during spring 2021 and both winters, except on 6-Apr-21 when <5 µm (e.g. 61% at H2) contributed more biomass than the two other size fractions combined (Fig. S6).

Mean Chl a concentrations were not significantly different between depths for either WLIS (T-test, p=0.07) or CLIS (T-test, p=0.94) (Fig. 5, S5, S6), though within WLIS notable differences were detected at both

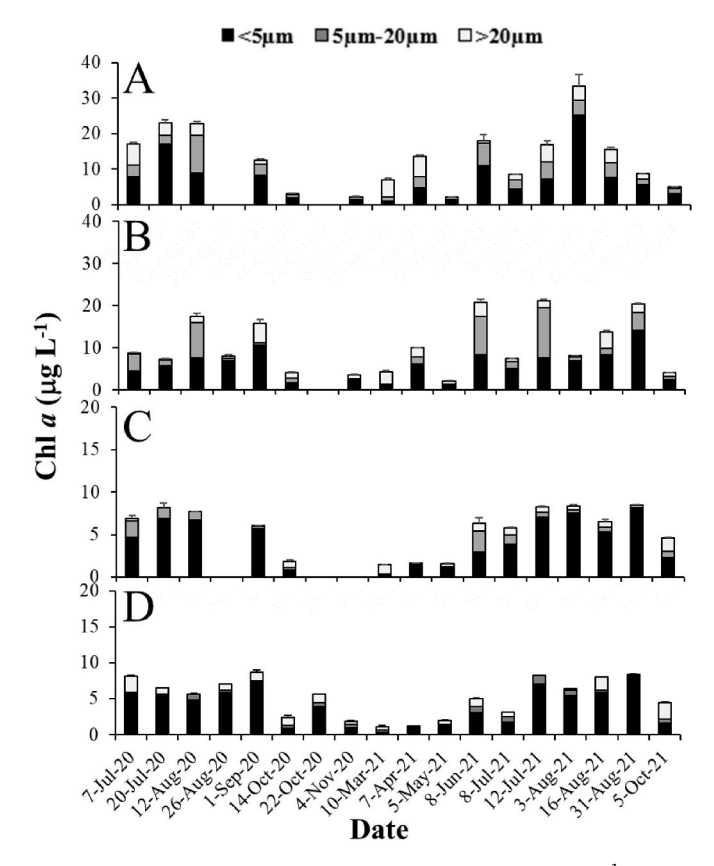


Fig. 6. Mean (n=3) (SE) Chlorophyll a (Chl a) concentrations (μ g L $^{-1}$) of three cell size fractions (>20 μ m, 5–20 μ m and <5 μ m) at 0.5 m depth in Western Long Island Sound (7-Jul-20 to 5-Oct-21) at stations A4 (A), B3 (B), C2 (C), and D3 (D). Error bars are for total Chl a. Note: different y-axis scales; x-axis depicts individual sampling dates, so temporal spacing between sampling dates vary.

A4 and B3 (Fig. 6, S5). For example, mean total Chl a on 3-Aug-21 was higher at 0.5 m (33.44 (5.39) μ g L⁻¹) than 2 m (25.76 (0.46) μ g L⁻¹), associated with an euglenoid bloom at 0.5 m (267 (0.84) cells mL⁻¹). In ELIS, Chl a concentrations at 2 m depth were significantly higher than 0.5 m throughout the study (T-test, p=0.002) (Figs. 2 and 3, S3). Discrete samples (2 m) were within 1 m of the SCM depth 47% of the time, and this was more common in WLIS based on CTD fluorescence profiles (Table S2), through cooler WLIS months ranged 3.0–6.5 m (Table S2). The SCM was deeper in CLIS and ELIS than WLIS, being above 10 m throughout the year with winter-spring SCM in ELIS generally at the deepest depths (~3–15 m) (Table S2).

3.4. Phytoplankton community composition

Of enumerated taxa, diatoms were the most abundant group throughout the study, especially during 2021, though abundances of flagellates (euglenoids, dinoflagellates, and nanoflagellates) increased during summers at WLIS (Fig. 7, S7, S8; Table S3). Diatoms bloomed both study years, but cell concentrations were generally lower during summer 2020 than summer 2021 when multiple diatom blooms (>300 cells $\mbox{mL}^{-1}\mbox{)}$ occurred at WLIS station A4; CLIS and ELIS cell concentrations remained <650 cells mL⁻¹ (Fig. 7, S7, S8; Table S3). The most commonly observed diatom genera were Leptocylindrus, Skeletonema, Chaetoceros, Thalassionema, and Thalassiosira, with other frequentlyobserved (at sub-bloom levels) genera including Amphiprora, Pleurosigma, Navicula, Asterionellopsis, and Odontella (Fig. 7, S7, S8; Table S3). The domoic-acid producing genus Pseudo-nitzschia spp. was observed in WLIS during 2021 at stations B3, C2, and D3 (3-Aug, 16-Aug) then again at C2 on 5-Oct. Among flagellates, euglenoids and Prorocentrum spp. were the most common WLIS taxa. Of the many Prorocentrum species

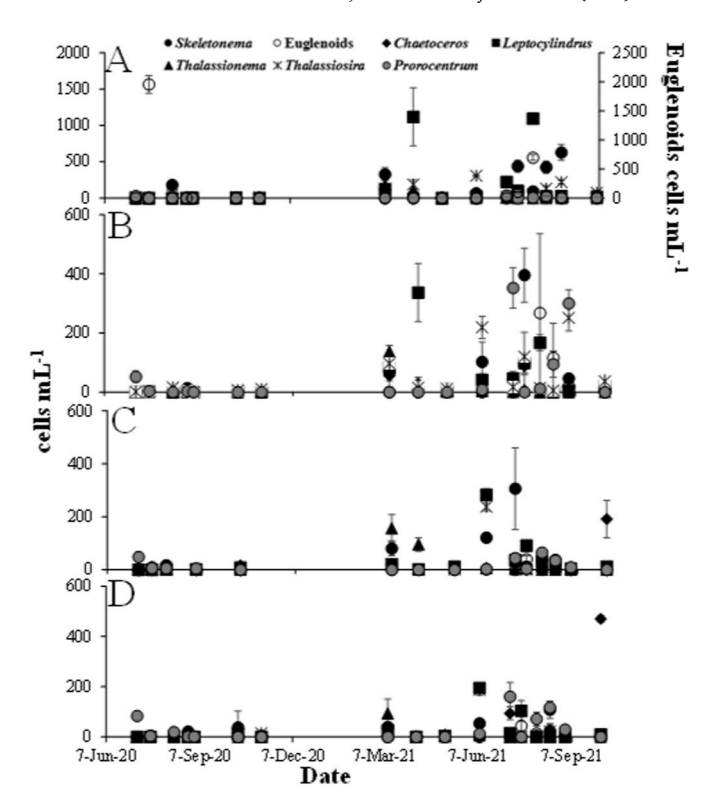


Fig. 7. Mean (n=3) (SE) cell concentrations (cells mL^{-1}) of most abundant microplankton genera at 0.5 m depth in Western Long Island (7-Jul-20 to 5-Oct-21) at stations A4 (A), B3 (B), C2 (C) and D3 (D). Note: different scale for euglenoids (secondary y-axis).

(*P. lima, P. triestinum, P. micans, P. triestinum,* and *P. minimum*) noted, *P. triestinum* was the most abundant and frequently observed, reaching mean (SD) concentrations of 352 (68) cells mL $^{-1}$, 8-Jul-21 at D3; *P. lima* and *P. minimum* concentrations remained \leq 89 cells mL $^{-1}$. Other HAB-forming dinoflagellates observed both summers in WLIS were *Dinophysis acuminata* and *Alexandrium* spp., both <10 cells mL $^{-1}$.

Phytoplankton population numbers exhibited considerable variability within WLIS and CLIS, despite the lack of significant seasonal differences between pooled Chl *a* means at sampled depths. WLIS and CLIS diatom abundances were comparable between depths (Fig. 7, S7, S8) whereas dinoflagellate cells, particularly *Prorocentrum*, as well as euglenoids were more frequently observed at 0.5 m than 2 m depth. For example, on 20-Jul-20 at A4, 1958 (153) cells mL⁻¹ euglenoids were counted at 0.5 m in contrast to 125 (43) cells mL⁻¹ at 2 m. By comparison, in ELIS diatom abundances were relatively higher at 2 m depth (Table S3).

3.5. PCA analysis

PC1 and PC2 together explained 53% of the data variation (31.3% and 21.7%, respectively). PC1 separated along a summer/fall to winter/spring axis whereas PC2 separated along a spring/summer to fall/winter axis, with seasons progressing in a clockwise direction around the biplot (Fig. 8). As expected, higher temperature loadings were associated with summer months whereas DO loadings were associated with winter months, consistent with reduced oxygen solubility in warmer waters. In particular, DIN, Si, PO_4^{3-} loadings (and DON, to a weak degree) were highly linked with fall months along the PC1 axis whereas the DOP loading was associated with summer months. Temperature and Chl a (<5 μm and 5–20 μm) were more closely tied to summer months along the PC2 axis. Chl a loadings from the <5 μm and 5–20 μm size fractions were associated with early-to mid-summer, whereas Chl a from the >20 μm size fraction showed no strong association with season.

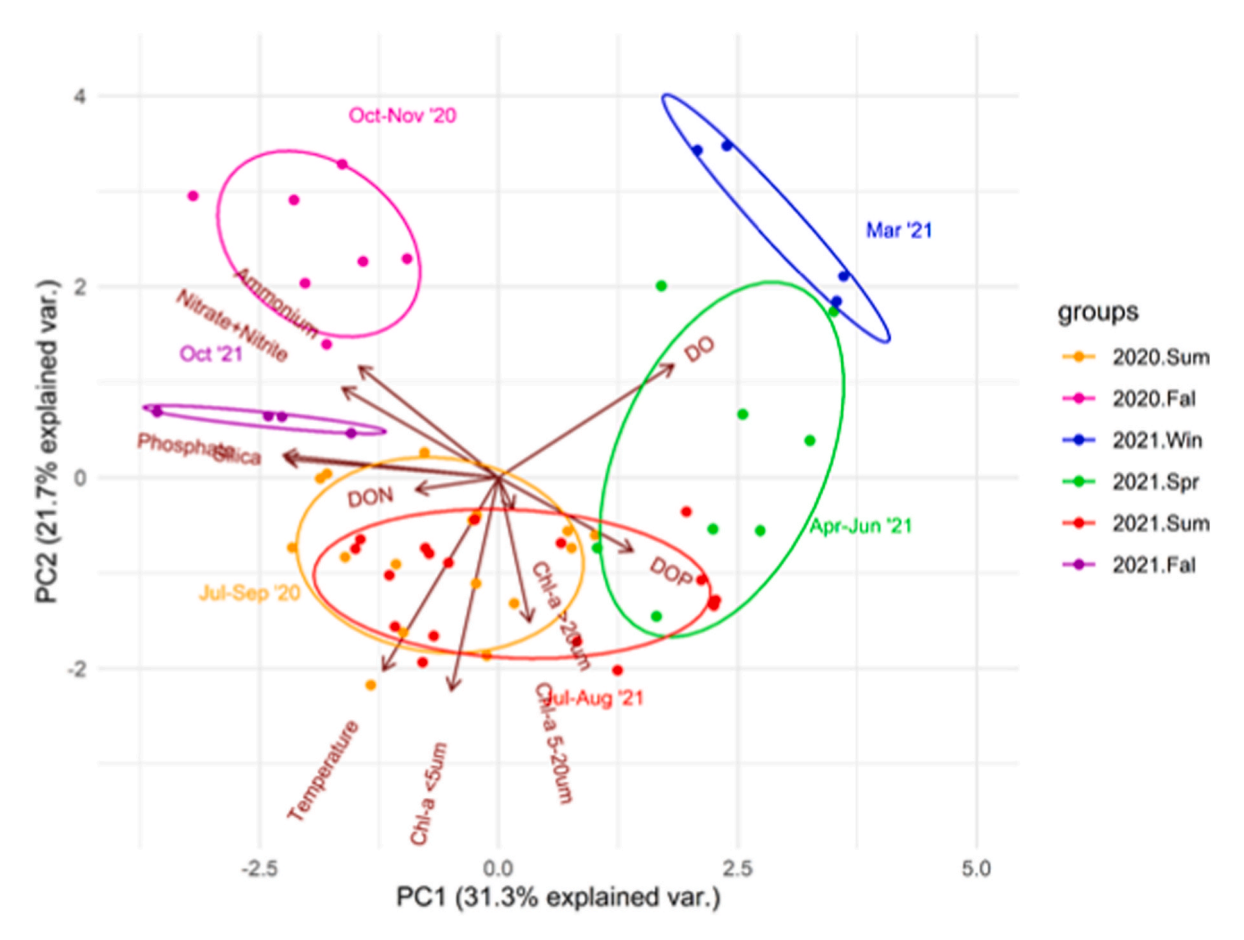


Fig. 8. PCA biplot for Western Long Island at 0.5 m depth showing PC scores and loadings between variables grouped by season: Summer 2020 (2020 Sum; orange; Jul–Sep'20), Fall 2020 (2020 Fal; pink; Oct to Nov'20), Winter 2021 (2021 Win; blue; Mar'21), Spring 2020 (2021 Spr; green; Apr–Jun'21), Summer 2021(2021 Sum; red; Jul–Aug'21) and Fall 2021 (2021 Fal; purple; Oct'21). Variables included: Chl a (>20 μ m, 20-5 μ m and <5 μ m), inorganic nutrients (nitrate + nitrite, ammonium, silica, and phosphate), temperature, and dissolved oxygen (DO). (For interpretation of the references to colour in this figure legend, the reader is referred to the Web version of this article.)

4. Discussion

4.1. Main findings

This study combined multiple physical and biogeochemical water quality parameters to evaluate seasonal phytoplankton community composition and biomass at spatial scales not recently assessed in LIS, providing new insight to ecological processes within this and similar urban estuaries. A clear west to east (urban to oceanic) transition in water quality and phytoplankton biomass was evident throughout the study, with concentrations of total Chl a and DIN decreasing west to east, consistent with prior work (Goebel et al., 2006; CTDEEP, 2021). These observations were coincident with a diminishing influence of urban, shallower, and less saline areas such as the Hudson River system to the relatively deeper, marine ecosystems (Gay et al., 2004; Lee and Lwiza, 2005; Vlahos et al., 2020). Flagellate abundances and smaller phytoplankton ($<5~\mu m$) biomass increased during summers in WLIS, with small nanoplankton and picoplankton typically contributing most to total Chl a in WLIS and CLIS, though microplankton (>20 µm) contributed most to total Chl a in ELIS. N form and concentration was directly connected to LIS seasonal phytoplankton biomass and community composition. For example, diatoms were abundant throughout both years with blooms associated with elevated $NO_3^- + NO_2^-$ whereas flagellates became numerous during summers when NH₄⁺ levels declined (Conover et al., 1954; Liu and Lin, 2008), indicating uptake. Low summer DIN concentrations could explain the elevated biomass of nanoplankton and picoplankton in WLIS since smaller cells with greater surface to volume ratios have a competitive advantage over larger ones in low DIN environments (Suter et al., 2014). Combined, these observations lay important groundwork for assessing the primary drivers of LIS phytoplankton species diversity.

4.2. Physical water quality

The similarity in seasonal means of phytoplankton biomass, nutrients and physical water quality parameters between study depths fallspring indicated that LIS surface waters (<2 m) were typically wellmixed during that time, facilitating comparable phytoplankton assemblages. During summer, differences in both total Chl a in ELIS and temperature across LIS developed along with seasonal thermoclines, indicating summer stratification of the water column (Lee and Lwiza, 2008; Wilson et al., 2008; Swanson et al., 2016). Concurrent (Jul 2020-Nov 2021) surveys of WLIS stations assessed herein reported thermocline and halocline development early June, with markedly warmer and fresher water in the upper 5 m (A4), 5-10 m (C2) and 10-20 m (B3, D3) (CTDEEP, 2020; Humphries et al., 2023). In CLIS, the summer thermocline was approximately 10 m with the exception of H6, where it formed closer to 20 m whereas in ELIS, a summer thermocline developed at I2 but pronounced stratification did not occur at other ELIS stations (CTDEEP, 2020). Halocline development followed the same trend as the thermocline in CLIS and ELIS. Stations with greater stratification likely enhanced the abundances and presumably growth rates of taxa such as dinoflagellates that thrive in warm, sub-surface waters due in part to their high respiration to maximal photosynthesis ratio

(Cushing, 1989; Pitcher et al., 1998) that potentially reduce summer DO levels. The generally increasing salinity gradient west to east was likely associated with freshwater inputs from the East River and Housatonic River to WLIS and CLIS relative to the strong marine exchange between the Atlantic Ocean and ELIS (Lee and Lwiza, 2005; Whitney, 2010; Li et al., 2018). DO levels (0.5 m and 2 m) increased during cooler seasons (spring and winter) then decreased during summers from reduced oxygen solubility in warmer waters (Staniec and Vlahos, 2017) and greater respiration, with recorded values (6–12 mg L⁻¹) comparable to prior studies (Anderson and Taylor, 2001; Staniec and Vlahos, 2017). Lastly, the extinction coefficient (*k*) was higher than previous work noting the 1% light attenuation ranging 5–11 m (Anderson and Taylor, 2001). This difference between extinction coefficients may be due to greater turbidity and/or currents that affected Secchi depth measurements.

4.3. Nutrients

Throughout the study, WLIS was characterized by higher DIN concentrations than either CLIS or ELIS (Goebel et al., 2006; Vlahos et al., 2020), consistent with the west receiving relatively more urban-sourced N (Vaudrey, 2017) and prior studies showing 2017 DIN concentrations higher at WLIS (A4) than ELIS (K2) (Vlahos et al., 2020). These data indicate that anthropogenic DIN inputs supported the relatively higher phytoplankton biomass measured in WLIS than the east (Anderson and Taylor, 2001; Anderson et al., 2008). DON was typically the greatest component of the dissolved N pool across LIS. DON may comprise up to 40% of LIS TN (Capriulo et al., 2002), as increasing DON stocks have been associated with rising TN levels despite DIN reductions (Suter et al., 2014). Wastewater treatment plants are a major source of anthropogenic DON because treatment of TN releases organic-N (Pehlivanoglu and Sedlak, 2004). In addition, the rising PO₄³⁻ concentrations during summers leading to higher fall levels differs from O'Shea and Brosnan (2000), where no seasonal trends in average PO₄³⁻ levels were observed in WLIS. Mean $NO_3^- + NO_2^-$ and PO_4^{3-} concentrations from this study were comparable to multi-year averages (2008-2016) in the Chesapeake Bay (Brush et al., 2020). The exception was fall 2021, when mean WLIS $NO_3^- + NO_2^-$ concentrations exceeded 10 μM such that the 5-Oct-21 spike coincided with a beach closure from unsafe Enterococcus levels (Riverkeeper.com 2022) indicating that elevated DIN and DON levels were at least partially caused by a CSO event. The rivers bordering LIS, such as the East River for WLIS and Connecticut River for ELIS, were likely major sources of N that contributed to the elevated $NO_3^- + NO_2^$ values observed here (Li et al., 2018; Vlahos et al., 2020).

4.4. Chlorophyll a

Over the study, elevated total Chl a during warmer temperatures (summers) were associated with greater proportions of picoplankton biomass and flagellate abundances compared to other phytoplankton taxa, supporting prior studies of LIS and regional phytoplankton communities (Greenfield et al., 2005; Goebel et al., 2006; Lonsdale et al., 2006; Rice and Stewart, 2013). By comparison, the absence of seasonal variability within the $>20 \mu m$ cell size fraction could have been due to colonial diatoms being constantly abundant throughout the study. Summers were also characterized by higher dinoflagellate numbers, including the HAB species P. minimum, P. triestinum, Alexandrium, and Dinophysis, whose growth rates and abundances are linked to surface temperatures (Heil et al., 2005; Flores-Moya et al., 2008; Kudela and Gobler, 2012; Gobler et al., 2017; Griffith et al., 2019b; Seto et al., 2019). Warmer temperatures (25-30 °C) also accelerate cell growth rates of the euglenoid Euglena gracilaris (Kitaya et al., 2005); these temperatures overlap the range of summer conditions in WLIS (19.67-26.85 °C) when euglenoid cell concentrations were high. Given predictions of increasing climate change-induced warming and stratification within LIS and globally, abundances of dinoflagellate (Rice and Stewart, 2013; Li et al., 2020) and euglenoid species could proliferate.

Consequently, abundances of HAB genera, such as *Dinophysis*, could become enhanced in the LIS mainstem and nearby embayments, creating a greater sanitation issue for shellfish aquaculture and recreational activities.

The west to east decline in total Chl a concentrations supported previous work (Goebel et al., 2006; Liu and Lin, 2008) and coincided with decreasing DIN levels. Within cell size fractions, the greatest contributor to Chl a in WLIS and CLIS was <5 µm (Greenfield et al., 2005; Lonsdale et al., 2006; Liu and Lin, 2008), and its eastward decrease paralleled diminishing DIN concentrations, indicating that DIN fuels WLIS picoplankton blooms. Abundances of the cyanobacterium Synechococcus can be elevated in CLIS and ELIS (Gobler et al., 2006; Latimer et al., 2014) though relatively scarce in WLIS (Gobler et al., 2006). However, during summer 2019 Santoferrera et al. (2022) detected both Synechococcus and Cyanobium, as well as the pelagophyte Aureococcus anophagefferens and the cryptophyte Plagioselmis prolonga (<5 μm), using 16S sequencing. This indicates that numerous small cell-size species inhabit WLIS and/or Synechococcus abundances have risen. In this study, the use of light microscopy limited the capability to accurately identify small phytoplankton, such as A. anophagefferens, that bloom in LIS embayments (Greenfield and Lonsdale, 2002; Gobler and Sunda, 2012) and in response to DON (Lomas et al., 2004; Nuzzi and Waters, 2004). The eastward decrease in the <5 µm cell size fraction could be affected by WLIS receiving more nutrient-rich and lower salinity riverine inputs, such as from the East River, than ELIS where the greater oceanic exchange facilitates diatom abundances. These inputs may also be why euglenoids, often considered indicators of water pollution, were abundant in WLIS (Li et al., 2018). Lastly, summer abundances of small (<7 μm) phytoplankton have been increasing in LIS over the past two decades with rising temperatures (Rice and Stewart, 2013; Suter et al., 2014; Gobler et al., 2017). This suggests that as coastal waters warm, picoplankton biomass can increase during the summer and/or their blooms may persist for longer periods of time within surface depths.

4.5. Phytoplankton community composition

Shifts in phytoplankton community composition were associated with N-form, especially DIN. Diatom abundances increased when $NO_3^ +\ NO_2^-$ concentrations were elevated, particularly during summer 2021 and falls. Most were centric chain forming genera such as Skeletonema, Leptocylindrus, Thalassiosira and Chaetoceros, in line with the affinity of LIS diatoms for NO₃ (George et al., 2014). Furthermore, the detection of Pseudo-nitzschia in 2021 here and in other HAB monitoring reports (Yarish et al., 2009; Van Gulick, 2020) indicates this toxigenic genus could pose a regional public health concern. Si levels were low when diatom abundances were high, such as winter-spring and summer of 2021, yet Si, $NO_3^- + NO_2^-$, and diatoms all increased in the fall. This demonstrates that Si and NO₃ + NO₂ co-regulate LIS diatom phenology (Gobler et al., 2006; George et al., 2014; Suter et al., 2014). In this study, high summer abundances of the dinoflagellate Prorocentrum typically coincided with elevated DON in WLIS, consistent with Prorocentrum spp. and other dinoflagellate genera effectively using DON (Glibert and Legrand, 2006; Bronk et al., 2007). Dinoflagellates are often abundant in areas of high DON and NH₄ concentrations (Kang and Kang et al., 2022), indicating that in LIS, DON favors dinoflagellate-dominated phytoplankton communities over diatom dominated ones. The higher values of NH₄⁺ compared to NO₃⁻ + NO₂⁻ during summer of 2020 could have further benefited dinoflagellates, as blooms of this taxon are frequently enhanced by both NH₄⁺ and warm temperatures (Hattenrath-Lehmann et al., 2010, 2015; Gobler and Hattenrath-Lehmann, 2011; Gobler et al., 2012), though blooms of the HAB species Alexandrium catenella and Dinophysis acuminata were not detected. This implies that while these species have a widespread distribution across LIS (Van Gulick, 2020), near-shore environments could be more conducive to their proliferation than the open water and should be taken into account for HAB

forecasting.

In terms of vertical trends within the water column, dinoflagellates and euglenoids were more abundant during summers and at 0.5 m depth than 2 m, coincident with warmer sub-surface layers and higher light (Figueiras and Pazos, 1991; Latasa et al., 2016b), though flagellate and dinoflagellate concentrations were comparable between depths when abundances were <25 cells mL⁻¹. By comparison, diatom abundances were similar among study depths, reflecting their capacity to span broad distributions and/or similar environmental conditions within the water column that both sustain diatom assemblages and enable luxury nutrient storage (Latasa et al., 2016a). The 2 m samples did not always overlap with the SCM, where diatom biomass tends to aggregate, so it is unclear whether diatom assemblages had further vertical delineations. However, across ELIS diatoms were often relatively more abundant at 2 m depths. This is likely at least partially attributed to its relatively lower extinction coefficient than WLIS (CTDEEP, 2021), which would enhance photosynthesis.

4.6. Conclusion

This project demonstrated how N, P, light, temperature, and salinity affect the spatial and temporal distributions of LIS phytoplankton community composition and biomass. Dinoflagellates and euglenoids became more abundant during summers with increasing temperatures, and diatom blooms often coincided with elevated NO₃ + NO₂ concentrations. While N form clearly influenced phytoplankton assemblage dynamics, Hypothesis 1 cannot be fully accepted because dinoflagellate blooms did not coincide with elevated NH₄⁺ concentrations. However, the decreasing west to east gradient of DIN concentrations coincident with lower total Chl a did support Hypothesis 1 and can be attributed to the declining urban to suburban gradient (NYC to the Atlantic Ocean). Hypothesis 2 was rejected due to similar mean water quality parameters between depths, with the exception of summer temperature and ELIS phytoplankton biomass. Rejection of Hypothesis 2 was based on the analysis of pooled mean values but does not account for dynamic, temporal changes that often characterize blooms.

This study was also impacted by COVID-19 such that water sampling and associated measurements were not permitted from mid Mar to Jun 2020, missing spring 2020 diatom blooms. Results also identified areas for subsequent research. For example, this study focused on 'bottom-up' (primarily nutrient) influences on phytoplankton assemblages, and data support dissolved N being a major driver of LIS biomass and species composition. However, 'top-down' (e.g., grazers, viruses) processes should be further explored, especially in the WLIS mainstem, because grazing influences phytoplankton assemblages in LIS and surrounding embayments (Lonsdale et al., 1996, 2006; Rice and Stewart, 2013; George et al., 2014), particularly under higher temperatures (George et al., 2014). Microzooplankton (ciliates and flagellates) can be more effective at grazing smaller phytoplankton cells than copepods (Sherr and Sherr, 2007; Sitta et al., 2018), but microzooplankton grazing rates may become outpaced by phytoplankton growth rates in nutrient enriched estuaries (Sitta et al., 2018). These studies indicate that as LIS becomes warmer and more N-enriched, zooplankton grazing rates and overall influence on phytoplankton communities may shift. Additionally, given the large contribution of small ($<5 \mu m$) phytoplankton to overall biomass, elucidating their species composition and abundances would help identify their ecological and biogeochemical roles within LIS.

In summary, diatom blooms coincided with elevated $NO_3^- + NO_2^-$ whereas dinoflagellate abundances were more closely linked with both NH_4^+ and temperature. Dinoflagellates, especially *P. triestinum*, were most abundant during the summer in WLIS while chain forming diatoms were abundant year-round across LIS. Most water quality parameters were similar between study depths, though dinoflagellates and other flagellates were noticeably more abundant in the warmer, 0.5 m depth, such as during summer stratification. There was a substantially greater

contribution of the <5 μm cell size fraction compared to other size classes in the west while larger phytoplankton (mostly diatoms) were the major biomass contributors in the east, coincident with a west to east gradient of decreasing DIN levels. This implies that future N-management decisions should re-evaluate TN targets to account for differences in DIN concentrations and phytoplankton biomass across LIS as climate change could exacerbate N-fueled phytoplankton productivity. Results from this study can be used to inform biogeochemical models, validate remote sensing efforts, and are likely broadly applicable to other urban estuaries worldwide.

CRediT authorship contribution statement

Zabdiel Roldan Ayala: Writing – original draft, Methodology, Investigation, Formal analysis, Data curation. Stephen A. Arnott: Writing – review & editing, Visualization, Validation, Software, Resources, Methodology, Formal analysis, Data curation. Mariapaola Ambrosone: Methodology, Formal analysis. Jessica I. Espinosa: Writing – review & editing, Methodology, Formal analysis. Georgie E. Humphries: Writing – review & editing, Methodology, Formal analysis. Maria Tzortziou: Writing – review & editing, Resources, Project administration, Funding acquisition, Conceptualization. Joaquim I. Goes: Writing – review & editing, Resources, Funding acquisition, Conceptualization. Dianne I. Greenfield: Writing – review & editing, Supervision, Resources, Project administration, Funding acquisition, Data curation, Conceptualization.

Declaration of competing interest

The authors declare that they have no known competing financial or other interests that influenced or could appear to have influenced data presented in this study.

Data availability

Data will be made available on request.

Acknowledgements

We gratefully thank the crew of the *R/V John Dempsey* with the Connecticut Department of Energy and Environmental Protection for help collecting water samples during their LIS surveys. Funding is courtesy of Environmental Protection Agency award #LI 96261317 Subaward # 82913/2/1156439, National Science Foundation awards DEB-2039867 and DEB-2039877, and the City University of New York (CUNY) - Advanced Science Research Center. JIG is also supported by NASA award NNH16ZDA001N-IDS and NOAA GST ST-1330-17-CQ-0050. We would also would like to thank members of the Greenfield Lab, Dr. Silvia Angles and Maximillian Brown as well as the Tzortziou Lab and Goes Lab for assisting in coordinating sampling trips, in addition to Queens College for the Queens College Masters Scholarship and Teaching Assistantships. Finally, we thank two anonymous reviewers who provided feedback on this manuscript.

Appendix A. Supplementary data

Supplementary data to this article can be found online at https://doi.org/10.1016/j.ecss.2023.108451.

References

Anderson, T.H., Taylor, G.T., 2001. Nutrient pulses, plankton blooms, and seasonal hypoxia in Western Long Island Sound. Estuaries 24 (2), 228–243. https://doi.org/10.2307/1352947.

Anderson, D.M., Burkholder, J., Cochlan, W.P., Glibert, P.M., Gobler, C.J., Heil, C.A., Kudela, R.M., Parsons, M.L., 2008. Harmful algal blooms and eutrophication:

- examining linkages from selected coastal regions of the United States. Harmful Algae 8 (1), $39–53.\ https://doi.org/10.1016/j.hal.2008.08.017.$
- Bates, D., Maechler, M., Bolker, B., Walker, S., 2015. Fitting linear mixed-effects models using lme4. J. Stat. Software 67 (1), 1–48. https://doi:10.18637/jss.v067.i01.
- Bennett, L.L., Thorpe, S.G., Guse, A.J., 2000. Cost-effective control of nitrogen loadings in Long Island Sound. Water Resour. Res. 36 (12), 3711–3720. https://doi.org/
- Bronk, D.A., See, J.H., Bradley, P., Killberg, L., 2007. DON as a source of bioavailable nitrogen for phytoplankton. Biogeosciences 4 (3), 283–296. https://doi.org/ 10.5194/bg.4-283-2007.
- Brown, M., Greenfield, D.I., 2022. Elucidating phytoplankton assemblage responses to nitrogen form following COVID-19 Stay-In-Place orders at the East River and Long Island Sound confluence. Tibor T. Polgar Fellowship Program, 2021. Section V:1-34 pp. In Yozzo, D.J., Fernald, S.H., Andreyko, H. (eds), Final Report.
- Brush, M.J., Mozetič, P., Francé, J., Aubry, F.B., Djakovac, T., Faganeli, J., Harris, L.A., Niesen, M., 2020. Phytoplankton dynamics in a changing environment. Geophys. Monogr. 49–74. https://doi.org/10.1002/9781119543626.ch4.
- Capriulo, G.M., Smith, G., Troy, R., Wikfors, G.H., Pellet, J., Yarish, C., 2002. The planktonic food web structure of a temperate zone estuary, and its alteration due to eutrophication. Hydrobiologia 475, 263–333. https://doi.org/10.1007/978-94-017-2464-7-73
- Connecticut Department of Energy and Environmental Protection (CTDEEP, Interstate Environmental Commission, US Environmental Protection Agency, 2020. 2021 Long Island Sound Hypoxia Season Review. Connecticut Department of Energy and Environmental Protection, Bureau of Water Protection and Land Reuse, Annual Report, p. 50.
- Connecticut Department of Energy and Environmental Protection (CTDEEP, Interstate Environmental Commission, US Environmental Protection Agency, 2021. 2021 Long Island Sound Hypoxia Season Review. Connecticut Department of Energy and Environmental Protection, Bureau of Water Protection and Land Reuse, Annual Report, p. 50.
- Conover, R., Riley, G., Deevin, G., Conover, S., Wheatland, S., Harrie, E., Sanders, H., 1954. Oceanography of long Island sound. Armed Services Technical Information Agency, Report 15, 421.
- Cullen, J.J., 2015. Subsurface chlorophyll maximum layers: enduring enigma or mystery solved? Ann. Rev. Mar. Sci 7 (1), 207–239. https://doi.org/10.1146/annurevmarine-010213-135111.
- Cushing, D.H., 1989. A difference in structure between ecosystems in strongly stratified waters and in those that are only weakly stratified. J. Plankton Res. 11 (1), 1–13. https://doi.org/10.1093/plankt/11.1.1.
- Figueiras, F.G., Pazos, Y., 1991. Microplankton assemblages in three bias Baixas (Vigo, Arosa and Muros, Spain) with a subsurface chlorophyll maximum: their relationships to hydrography. Mar. Ecol. Prog. Ser. 76, 219–233. https://doi.org/10.3354/meps/76219
- Flores-Moya, A., Costas, E., López-Rodas, V., 2008. Roles of adaptation, chance and history in the evolution of the dinoflagellate *Prorocentrum triestinum*. Naturwissenschaften 95 (8), 697–703. https://doi.org/10.1007/s00114-008-0372-1.
- Gay, P.S., O'Donnell, J., Edwards, C.A., 2004. Exchange between Long Island Sound and adjacent waters. J. Geophys. Res.: Oceans 109 (C6), 1–15. https://doi.org/10.1029/ 2004JC002319.
- George, J.A., Lonsdale, D.J., Merlo, L.R., Gobler, C.J., 2014. The interactive roles of temperature, nutrients, and zooplankton grazing in controlling the winter-spring phytoplankton bloom in a temperate, coastal ecosystem, Long Island Sound. Limnol. Oceanogr. 60 (1), 110–126. https://doi.org/10.1002/lno.10020.
- Glibert, P.M., Legrand, C., 2006. The diverse nutrient strategies of harmful algae: focus on osmotrophy. Ecology of Harmful Algae 189, 163–175. https://doi.org/10.1007/ 978-3-540-32210-8 13.
- Gobler, C., Hattenrath-Lehmann, T., 2011. The Distribution, Causes, and Impacts of Alexandrium Fundyense Blooms in Coves, Near Shore, and Open Water Regions of Long Island Sound. Long Island Sound Study, p. 21. Report.
- Gobler, C.J., Sunda, W.G., 2012. Ecosystem disruptive algal blooms of the brown tide species, Aureococcus anophagefferens and Aureoumbra lagunensis. Harmful Algae 14, 36–45. https://doi.org/10.1016/j.hal.2011.10.013.
- Gobler, C.J., Buck, N.J., Sieracki, M.E., Sañudo-Wilhelmy, S.A., 2006. Nitrogen and silicon limitation of phytoplankton communities across an urban estuary: the East River-Long Island Sound System. Estuar. Coast Shelf Sci. 68 (1–2), 127–138. https:// doi.org/10.1016/j.ecss.2006.02.001.
- Gobler, C.J., Burson, A., Koch, F., Tang, Y., Mulholland, M.R., 2012. The role of nitrogenous nutrients in the occurrence of harmful algal blooms caused by *Cochlodinium polykrikoides* in New York Estuaries (USA). Harmful Algae 17, 64–74. https://doi.org/10.1016/j.hal.2012.03.001.
- Gobler, C.J., Doherty, O.M., Hattenrath-Lehmann, T.K., Griffith, A.W., Kang, Y., Litaker, R.W., 2017. Ocean warming since 1982 has expanded the niche of toxic algal blooms in the North Atlantic and North Pacific Oceans. Proc. Natl. Acad. Sci. USA 114 (19), 4975–4980. https://doi.org/10.1073/pnas.1619575114.
- Goebel, N.L., Kremer, J.N., Edwards, C.A., 2006. Primary production in Long Island Sound. Estuar. Coast 29 (2), 232–245. https://doi.org/10.1007/bf02781992.
- Grasshoff, K.K., Kremling, K., Ehrhardt, M., 1999. Methods of Seawater Analysis. Wiley-VCH, p. 599.
- Greenfield, D.I., Lonsdale, D.J., 2002. Mortality and growth of juvenile hard clams Mercenaria mercenaria during brown tide. Mar. Biol. 141 (6), 1045–1050. https://doi.org/10.1007/s00227-002-0890-x.
- Greenfield, D.I., Lonsdale, D.J., Cerrato, R.M., 2005. Linking phytoplankton community composition with juvenile-phase growth in the Northern Quahog Mercenaria mercenaria (L.). Estuaries 28 (2), 241–251. https://doi.org/10.1007/bf02732858.

- Griffith, A.W., Doherty, O.M., Gobler, C.J., 2019a. Ocean warming along temperate western boundaries of the Northern Hemisphere promotes an expansion of *Cochlodinium polykrikoides* blooms. Proc. Biol. Sci. 286 (1904), 20190340 https://doi.org/10.1098/rspb.2019.0340.
- Griffith, A.W., Shumway, S.E., Gobler, C.J., 2019b. Differential mortality of North Atlantic bivalve molluscs during harmful algal blooms caused by the dinoflagellate, Cochlodinium (a.k.a. Margalefidinium) polykrikoides. Estuar. Coast 42 (1), 190–203. https://doi.org/10.1007/s12237-018-0445-0.
- Hattenrath- Lehmann, T.K., Anderson, D.M., Gobler, C.J., 2010. The influence of anthropogenic nitrogen loading and meteorological conditions on the dynamics and toxicity of *Alexandrium fundyense* blooms in a New York (USA) estuary. Harmful Algae 9 (4), 402–412. https://doi.org/10.1016/j.hal.2010.02.003.
- Hattenrath-Lehmann, T.K., Marcoval, M.A., Mittlesdorf, H., Goleski, J.A., Wang, Z., Haynes, B., Morton, S.L., Gobler, C.J., 2015. Nitrogenous nutrients promote the growth and toxicity of *Dinophysis acuminata* during estuarine bloom events. PLoS One 10 (4). https://doi.org/10.1371/journal.pone.0124148.
- Heil, C.A., Glibert, P.M., Fan, C., 2005. Prorocentrum minimum (Pavillard) Schiller: a review of a harmful algal bloom species of growing worldwide importance. Harmful Algae 4 (3), 449–470. https://doi.org/10.1016/j.hal.2004.08.003.
- Heil, C.A., Revilla, M., Glibert, P.M., Murasko, S., 2007. Nutrient quality drives differential phytoplankton community composition on the Southwest Florida Shelf. Limnol. Oceanogr. 52 (3), 1067–1078. https://doi.org/10.4319/lo.2007.52.3.1067.
- Heisler, J., Glibert, P.M., Burkholder, J.M., Anderson, D.M., Cochlan, W., Dennison, W. C., Dortch, Q., Gobler, C.J., Heil, C.A., Humphries, E., Lewitus, A., Magnien, R., Marshall, H.G., Sellner, K., Stockwell, D.A., Stoecker, D.K., Suddleson, M., 2008. Eutrophication and harmful algal blooms: a scientific consensus. Harmful Algae 8, 3–13. https://doi.org/10.1016/j.hal.2008.08.006.
- Humphries, G.E., Espinosa, J.I., Ambrosone, M., Roldan Ayala, Z., Tzortziou, M., Goes, J., Greenfield, D.I., 2023. Transitions in nitrogen and organic matter form and concentration correspond to bacterial population dynamic in a hypoxic urban estuary. Biogeochemistry 163, 219–243. https://doi.org/10.1007/s10533-023-01021-2.
- Kang, Y., Kang, C.-K., 2022. Reduced forms of nitrogen control the spatial distribution of phytoplankton communities: the functional winner, dinoflagellates in an anthropogenically polluted estuary. Mar. Pollut. Bull. 177, 113528 https://doi.org/ 10.1016/j.marpolbul.2022.113528.
- Kitaya, Y., Azuma, H., Kiyota, M., 2005. Effects of temperature, CO2/O2 concentrations and light intensity on cellular multiplication of microalgae, *Euglena gracilis*. Adv. Space Res. 35 (9), 1584–1588. https://doi.org/10.1016/j.asr.2005.03.039.
- Krauter, J.N., Klinck, J., Powell, E.M., Hofmann, E.E., Buckner, S., Grizzle, R., Bricelj, V. M., 2009. Effects of the fishery on the northern quahog (=hard clam, Mercenaria mercenaria L.) population in Great South Bay, New York: a modeling study.
 J. Shellfish Res. 27 (4), 653–666. https://doi.org/10.2983/0730-8000(2008)27.
- Kudela, R.M., Gobler, C.J., 2012. Harmful dinoflagellate blooms caused by Cochlodinium sp.: global expansion and ecological strategies facilitating bloom formation. Harmful Algae 14, 71–86. https://doi.org/10.1016/j.hal.2011.10.015.
- Lachat Instruments, 2019. Methods List for Automated Ion Analyzers. Manual, 52 pp. Latasa, M., Cabello, A.M., Morán, X.A., Massana, R., Scharek, R., 2016a. Distribution of phytoplankton groups within the deep chlorophyll maximum. Limnol. Oceanogr. 62 (2), 665–685. https://doi.org/10.1002/lno.10452.
- Latasa, M., Gutiérrez-Rodríguez, A., Cabello, A.M., Scharek, R., 2016b. Influence of light and nutrients on the vertical distribution of marine phytoplankton groups in the deep chlorophyll maximum. Sci. Mar. 80 (S1), 57–62. https://doi.org/10.3989/ scimar.04316.01a.
- Latimer, J.S., Tedesco, M.A., Swanson, R.L., Yarish, C., Stacey, P.E., Garza, C., 2014. Long Island Sound, Prospects for the Urban Sea. Springer, p. 558.
- Lee, Y.J., Lwiza, K., 2005. Interannual variability of temperature and salinity in shallow water: Long Island Sound, New York. J. Geophys. Res. 110 (C9), 1–12. https://doi. org/10.1029/2004ic002507.
- Lee, Y.J., Lwiza, K., 2008. Characteristics of bottom dissolved oxygen in Long Island Sound, New York. Estuar. Coast Shelf Sci. 76 (2), 187–200. https://doi.org/10.1016/ j.ecss.2007.07.001.
- LeGresley, M., McDermott, G., 2010. Counting chamber methods for quantitative phytoplankton analysis - haemocytometer, Palmer-Maloney cell and Sedgewick-Rafter cell. Intergovernmental Oceanographic Commission manuals and guides 55: Microscopic and molecular methods for quantitative phytoplankton analysis. JINESCO 25–30
- Lenth, R., 2022. Estimated marginal means, aka least-squares means. R package version 1.7.4-1. URL. https://CRAN.R-project.org/package=emmeans.
- Li, Y., Meseck, S.L., Dixon, M.S., Wikfors, G.H., 2018. The East river tidal strait, New York city, New York, a high-nutrient, low-chlorophyll coastal system. Int. Aquat. Res. 10 (1), 65–77. https://doi.org/10.1007/s40071-018-0189-2.
- Li, G., Cheng, L., Zhu, J., Trenberth, K.E., Mann, M.E., Abraham, J.P., 2020. Increasing ocean stratification over the past half-century. Nat. Clim. Change 10 (12), 1116–1123. https://doi.org/10.1038/s41558-020-00918-2.
- Liu, S., Lin, S., 2008. Temporal and spatial variation of phytoplankton community in Long Island Sound. In: 9th Biannual Long Island Sound Conference Proceedings, pp. 28–34.
- Lomas, M.W., Kana, T.M., MacIntyre, H.L., Cornwell, J.C., Nuzzi, R., Waters, R., 2004. Interannual variability of Aureococcus anophagefferens in Quantuck Bay, Long Island: natural test of the DON hypothesis. Harmful Algae 3 (4), 389–402. https://doi.org/10.1016/j.hal.2004.06.009.
- Lonsdale, D.J., Cosper, E.M., Doall, M., 1996. Effects of zooplankton grazing on phytoplankton size-structure and biomass in the Lower Hudson River Estuary. Estuaries 19 (4), 874–889. https://doi.org/10.2307/1352304.

- Lonsdale, D.J., Greenfield, D.I., Hillebrand, E.M., Nuzzi, R., Taylor, G.T., 2006.
 Contrasting microplanktonic composition and food web structure in two coastal embayments (Long Island, NY, USA). J. Plankton Res. 28 (10), 891–905. https://doi.org/10.1093/plankt/fbl027.
- Mariani, P., Andersen, K.H., Visser, A.W., Barton, A.D., Kiørboe, T., 2013. Control of plankton seasonal succession by adaptive grazing. Limnol. Oceanogr. 58 (1), 173–184. https://doi.org/10.4319/lo.2013.58.1.0173.
- New York State Department of Environmental Conservation (NYSDEC), Connecticut Department of Environmental Protection (CTDEEP), 2000. A Total Maximum Daily Load Analysis to Achieve Water Quality Standards for Dissolved Oxygen in Long Island Sound. Report, p. 73.
- Nuzzi, R., Waters, R.M., 2004. Long-term perspective on the dynamics of brown tide blooms in Long Island coastal bays. Harmful Algae 3 (4), 279–293. https://doi.org/ 10.1016/j.hal.2004.04.001.
- O'Shea, M.L., Brosnan, T.M., 2000. Trends in indicators of eutrophication in western Long Island Sound and the Hudson-Raritan Estuary. Estuaries 23 (6), 877–901. https://doi.org/10.2307/1353004.
- Parker, C.A., O'Reilly, J.E., 1991. Oxygen depletion in Long Island Sound: a historical perspective. Estuaries 14 (3), 248–264. https://doi.org/10.2307/1351660.
- Parsons, T.R., Maita, Y., Lalli, C.M., 1984. A Manual of Chemical and Biological Methods for Seawater Analysis. Pergamon Press, p. 173.
- Pehlivanoglu, E., Sedlak, D.L., 2004. Bioavailability of wastewater-derived organic nitrogen to the alga Selenastrum Capricornutum. Water Res. 38 (14–15), 3189–3196. https://doi.org/10.1016/j.watres.2004.04.027.
- Pitcher, G.C., Boyd, A.J., Horstman, D.A., Mitchell-Innes, B.A., 1998. Subsurface dinoflagellate populations, frontal blooms and the formation of red tide in the Southern Benguela upwelling system. Mar. Ecol. Prog. Ser. 172, 253–264. https:// doi.org/10.3354/meps172253.
- R Core Team, 2022. R: A Language and Environment for Statistical Computing. R
 Foundation for Statistical Computing, Vienna, Austria. URL. https://www.R-project.org.
- R Studio Team, 2022. RStudio: integrated development environment for R. RStudio, PBC, boston, MA, URL, http://www.rstudio.com.
- Rice, E., Stewart, G., 2013. Analysis of interdecadal trends in chlorophyll and temperature in the central basin of Long Island Sound. Estuar. Coast Shelf Sci. 128, 64–75. https://doi.org/10.1016/j.ecss.2013.05.002.
- Riverkeeper.com, 2022. East River mid-channel at Roosevelt Island Entero/Rainfall Table. Riverkeeper. https://www.riverkeeper.org/water-quality/hudson-river/nyc-hudson-bergen/east-river-midchannel-roosevelt/.
- Santoferrara, L.F., McManus, G.B., Greenfield, D.I., Smith, S.A., 2022. Microbial Communities (bacteria, Archaea and eukaryotes) in a temperate estuary during seasonal hypoxia. Aquat. Microb. Ecol. 88, 61–79. https://doi.org/10.3354/ ame01982.
- Seto, D.S., Karp-Boss, L., Wells, M.L., 2019. Effects of increasing temperature and acidification on the growth and competitive success of *Alexandrium catenella* from the Gulf of Maine. Harmful Algae 89, 101670. https://doi.org/10.1016/j. hal.2019.101670.
- Sherr, E.B., Sherr, B.F., 2007. Heterotrophic dinoflagellates: a significant component of microzooplankton biomass and major grazers of diatoms in the sea. Mar. Ecol. Prog. Ser. 352, 187–197. https://doi.org/10.3354/meps07161.
- Sitta, K., Callahan, T., Doll, C., Mortensen, R., Reed, M., Greenfield, D.I., 2018. The influences of nitrogen form and zooplankton grazing on phytoplankton assemblages in two coastal southeastern systems. Limnol. Oceanogr. 63, 2523–2544. https://doi. org/10.1002/lno.10957.
- Staniec, A., Vlahos, P., 2017. Timescales for determining temperature and dissolved oxygen trends in the Long Island Sound (LIS) estuary. Continent. Shelf Res. 151, 1–7. https://doi.org/10.1016/j.csr.2017.09.013.

- Suter, E.A., Lwiza, K.M.M., Rose, J.M., Gobler, C., Taylor, G.T., 2014. Phytoplankton assemblage changes during decadal decreases in nitrogen loadings to the urbanized Long Island Sound Estuary, USA. Mar. Ecol. Prog. Ser. 497, 51–67. https://doi.org/ 10.3354/mens/0602
- Swanson, R.L., Bauer, C.L., Wilson, R.E., Rose, P.S., O'Connell, C., 2016. Physical processes contributing to localized, seasonal hypoxic conditions in the bottom waters of Smithtown Bay, Long Island Sound, New York. J. Coast Res. 317, 91–104. https://doi.org/10.2112/jcoastres-d-14-00118.1.
- Tamborski, J.J., Cochran, J.K., Bokuniewicz, H.J., 2017. Submarine groundwater discharge driven nitrogen fluxes to long Island sound, NY: terrestrial vs. Marine sources. Geochem. Cosmochim. Acta 218, 40–57. https://doi.org/10.1016/j. 972.2017.09.003
- Tossavainen, M., Ilyass, U., Ollilainen, V., Valkonen, K., Ojala, A., Romantschuk, M., 2019. Influence of long-term nitrogen limitation on lipid, protein and pigment production of *Euglena gracilis* in photoheterotrophic cultures. PeerJ 7, e6624. https://doi.org/10.7717/peerj.6624.
- US Census Bureau, 2020. QuickFacts Connecticut and New York. U.S. Census Bureau. https://www.census.gov/quickfacts/CT.
- Van Gulick, E.V., 2020. 2020 Connecticut Harmful Algal Bloom Report. Department of Agriculture, Report, p. 65.
- Vaudrey, J.M., 2017. Thesis. In: New York City's Impact on Long Island Sound Water Quality. University of Connecticut, p. 33.
- Venables, W.N., Ripley, B.D., 2002. Modern Applied Statistics with S, fourth ed. Springer, p. 497
- Vlahos, P., Whitney, M.M., Menniti, C., Mullaney, J.R., Morrison, J., Jia, Y., 2020. Nitrogen budgets of the Long Island Sound estuary. Estuar. Coast Shelf Sci. 232, 106493 https://doi.org/10.1016/j.ecss.2019.106493.
- Welschmeyer, N.A., 1994. Fluorometric analysis of chlorophyll a in the presence of chlorophyll b and pheopigments. Limnol. Oceanogr. 39 (8), 1985–1992. https://doi. org/10.4319/lo.1994.39.8.1985.
- Whitney, M.M., 2010. A study on river discharge and salinity variability in the middle atlantic bight and long Island sound. Continent. Shelf Res. 30 (3–4), 305–318. https://doi.org/10.1016/j.csr.2009.11.011.
- Whitney, M.M., Vlahos, P., 2021. Reducing hypoxia in an urban estuary despite climate warming. Environ. Sci. Technol. 55 (2), 941–951. https://doi.org/10.1021/acs. est.0c03964.s001.
- Wikfors, G.H., 2005. A review and new analysis of trophic interactions between *Prorocentrum minimum* and clams, scallops, and oysters. Harmful Algae 4 (3), 585–592. https://doi.org/10.1016/j.hal.2004.08.008.
- Wilson, R.E., Swanson, R.L., Crowley, H.A., 2008. Perspectives on long-term variations in hypoxic conditions in western Long Island Sound. J. Geophys. Res.: Oceans 113 (C12), 1–13. https://doi.org/10.1029/2007jc004693.
- Wolfe, D.A., Monahan, R., Stacey, P.E., Farrow, D.R., Robertson, A., 1991. Environmental quality of Long Island Sound: assessment and management issues. Estuaries 14 (3), 224–236. https://doi.org/10.2307/1351658.
- Yarish, C., Whilatch, R., Kraemer, G., Lin, S., 2009. Multi-component evaluation to minimize the spread of aquatic invasive seaweeds, harmful algal bloom microalgae, and invertebrates via the live bait vector in Long Island Sound. University of Connecticut, OpenCommons@UConn, p. 20.
- Zajac, R.N., Stefaniak, L.M., Babb, I., Conroy, C.W., Penna, S., Chadi, D., Auster, P.J., 2020. Chapter 10 - an integrated seafloor habitat map to inform marine spatial planning and management: a case study from Long Island Sound (Northwest Atlantic). Seafloor Geomorphology as Benthic Habitat 199–217. https://doi.org/ 10.1016/b978-0-12-814960-7.00010-5, 2nd ed.